Title

A multi-cohort genome-wide association study in African ancestry individuals reveals risk loci for primary open-angle glaucoma

Journal

Cell, 187(2)

ISSN

0092-8674

Authors

Verma, Shefali S

Gudiseva, Harini V

Chavali, Venkata RM

et al.

Publication Date

2024

DOI

10.1016/j.cell.2023.12.006

Peer reviewed

HHS Public Access

Author manuscript

Cell. Author manuscript; available in PMC 2025 February 21.

Published in final edited form as:

Cell. 2024 January 18; 187(2): 464–480.e10. doi:10.1016/j.cell.2023.12.006.

A multi-cohort genome-wide association study in African ancestry individuals reveals risk loci for primary open-angle glaucoma

A full list of authors and affiliations appears at the end of the article.

SUMMARY

Primary open-angle glaucoma (POAG), the leading cause of irreversible blindness worldwide, disproportionately affects individuals of African ancestry. We conducted a genome-wide association study (GWAS) for POAG in 11,275 individuals of African ancestry (6,003 cases; 5,272 controls). We detected 46 risk loci associated with POAG at genome-wide significance. Replication and post-GWAS analyses, including functionally informed fine-mapping, multiple trait co-localization, and *in silico* validation, implicated two previously undescribed variants (rs1666698 mapping to *DBF4P2*; rs34957764 mapping to *ROCK1P1*) and one previously associated variant (rs11824032 mapping to *ARHGEF12*) as likely causal. For individuals of African ancestry, a polygenic risk score (PRS) for POAG from our mega-analysis (African ancestry individuals) outperformed a PRS from summary statistics of a much larger GWAS derived from European ancestry individuals. This study quantifies the genetic architecture similarities and differences between African and non-African ancestry populations for this blinding disease.

Graphical abstract

*Correspondence: joan.o'brien@pennmedicine.upenn.edu.

AUTHOR CONTRIBUTIONS

Conceptualization: S.S.V., H.V.G., M.D.R., and J.M.O.; methodology: S.S.V., H.V.G., V.R.M.C., M.D.R., and J.M.O.; software: S.S.V., H.V.G., Y.B., L.G., A.L., M.D.R., and J.M.O.; validation: S.S.V., H.V.G., B.Z., A.S.B., C.P.M., M.C.Z., S.M.W., J.C.B., J.I.R., R.W., C.C.K., M.A.H., M.D.R., and J.M.O.; formal analysis: S.S.V., H.V.G., Y.B., M.P., G.-s.Y., M.D.R., and J.M.O.; investigation: S.S.V., H.V.G., V.R.M.C., R.J.S., D.W.C., V.V., R.M.N., S.R., J.H., R.L., S.Z.-G., A.S.B., N.K., E.D., W.M., J.H., Regeneron Genetics Center, T.G.K., S.K.I., N.S.P., VA Million Veteran Program, K.D.T., X.G., Y.-D.I.C., L.Z., C.G., R.A., J.L.W., C.M.C.-O., S.E.W., S.A., D.L.B., O.O.O., M.R., A.A., O.M.A., T.A., J.L.W., A.G.R., Q.N.C., V.A., A.L., E.M.-E., P.S.S., J.C.B., J.I.R., R.W., C.C.K., M.A.H., M.D.R., and J.M.O.; resources: M.D.R. and J.M.O.; data curation: R.L., E.D., M.D.R., and J.M.O.; writing – original draft: S.S.V., H.V.G., V.R.M.C., and R.J.S.; writing – review & editing: all authors; visualization: S.S.V., H.V.G., V.R.M.C., Y.B., V.V., M.D.R., and J.M.O.; supervision: M.D.R. and J.M.O.; project administration: S.S.V., H.V.G., R.J.S., M.D.R., and J.M.O.; funding acquisition: M.D.R. and J.M.O.

SUPPLEMENTAL INFORMATION

Supplemental information can be found online at https://doi.org/10.1016/j.cell.2023.12.006.

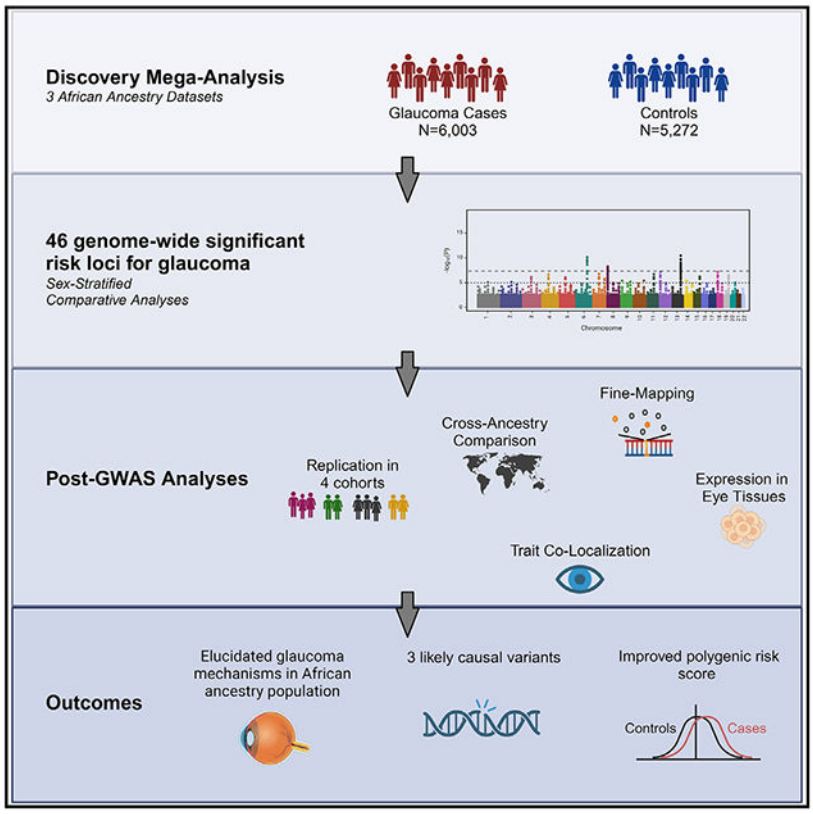

In brief

Glaucoma represents a pressing public health need among African ancestry individuals. This study provides novel insight into the genetic architecture of glaucoma in this population by identifying gene variants with pathophysiological significance.

INTRODUCTION

Primary open-angle glaucoma (POAG) is an insidious neurodegenerative disease of the optic nerve (ON) that causes progressive loss of peripheral vision.[1] This disease affects 44 million individuals worldwide, with a projected prevalence of 80 million by 2040.[2] It is estimated that 6 million individuals were bilaterally blinded by POAG in 2020.[3] African ancestry populations worldwide are disproportionately affected by this disease.[3] Individuals of African ancestry are four to five times more likely to be affected by POAG than individuals of European ancestry[4] and up to 15 times more likely to experience vision loss from the disease.[5]

There are several major risk factors for POAG in all populations, including advanced age, elevated intraocular pressure (IOP), and family history of glaucoma, with heritability estimates ranging from 0.17 to 0.81.[6] Elevated IOP is currently the only targetable component of the disease, and treatments are often ineffective in halting disease progression.[7,8] Additionally, some patients maintain normal IOP levels (normal-tension glaucoma) but can still experience disease progression and vision loss.[9] This indicates that

POAG, a frequently inherited disease, has additional underlying mechanisms that could be elucidated by genetic studies.[10,11]

Despite POAG having a strong inherited component,[12–15] understanding of the disease's genetics remains incomplete.[16] A total of 174 unique risk loci have been associated with POAG and related traits through a large-scale meta-analysis[17] and genome-wide association studies (GWASs) in European,[18–22] Japanese,[23–27] or multi-ancestry populations,[22,28,29] with sample sizes ranging from 387 to 383,500. However, many of these loci have a reduced or unknown role in individuals of African ancestry, indicating that global ancestry groups may have differences in genetic risk and highlighting the need to compare diverse genetic architectures.[29–32]

Several studies have investigated glaucoma genetics in multiancestry or African ancestry populations but were often limited by a small sample size.[33,34] One GWAS of continental African and African American populations identified a previously undescribed candidate locus on the *EXOC4* gene, but it did not associate in the West African replication group.[31] The African Descent and Glaucoma Evaluation Study (ADAGES)[35] identified an association with advanced POAG and the *ENO4* locus.[36] Most recently, a GWAS in the Genetics of Glaucoma in People of African Descent (GGLAD) consortium identified a previously undescribed locus in *APBB2* as significantly associated with POAG in individuals of African ancestry, but the index variant (rs59892895) was not polymorphic in participants of European or Asian ancestry.[37]

In this study, we conducted a large GWAS for POAG in African ancestry individuals from three African population datasets. We further investigated significant findings through replication studies in four independent datasets, functional validation studies, and *in silico* analysis. We also compared the genetic architecture of POAG in African and non-African ancestry populations. Our objective was to identify variants of pathophysiological importance to POAG in African ancestry individuals, gaining insight into the genetics of this blinding familial disease in the most affected population.

RESULTS

Study datasets

We performed a mega-analysis in a discovery cohort that combined three African ancestry datasets: the ADAGES study (n = 1,999),[36] the GGLAD consortium (n = 2,952),[37] and the Primary Open-Angle African American Glaucoma Genetics (POAAGG) study (n = 6,324)[38] (Figure 1). Genotype data were imputed for each dataset individually using the Trans-Omics for Precision Medicine (TOPMED) reference panel.[39]

The results from the discovery analysis were replicated in four independent datasets of African ancestry individuals: a second independent dataset from GGLAD (referred to as GGLAD-2),[37] All of Us (AOU),[40] Penn Medicine BioBank (PMBB),[41] and Million Veteran Program (MVP).[42] Additionally, we compared the results from the discovery mega-analysis with multi-ancestry GWAS results from the Global Biobank Meta-Analysis Initiative (GBMI)[17] and the National Human Genome Reserach Institute-European Bioinformatics

Institute (NHGRI-EBI) GWAS Catalog.[43] Finally, we created a polygenic risk score (PRS), which was applied to three independent datasets of African ancestry individuals (Electronic Medical Records and Genomics [eMERGE], n = 13,493; GGLAD-2, n = 1,490; PMBB, n = 11,117). The demographics and designs of the studies used in these analyses are detailed in Figure 1.

Discovery of known and previously undescribed POAG loci

In the discovery mega-analysis, all subjects had self-reported African ancestry or were recruited from continental Africa, and 51.5% were female (Figure 1). In total, 12,944,299 variants were included in the discovery analyses (STAR Methods). Correlation analyses revealed a generally high positive correlation (Figure S1A) between mega-analysis and meta-analysis results, indicating a strong agreement between the two approaches (Pearson correlation coefficient = 0.86). This finding suggests that both methods yield consistent findings overall. Furthermore, to investigate the power of the mega-analysis approach, we focused on variants filtered at a p value threshold of 1×10^{-04} (Figure S1B). Notably, we observed that smaller effect sizes in our mega-analysis exhibited higher p values, indicating higher power to detect these variants. These results highlight the robustness and statistical power of the mega-analysis approach employed in this study. Moreover, the observation that smaller effect sizes had higher power in the mega-analysis emphasizes the advantages of pooling individual-level data when possible to increase the precision and sensitivity of our analysis.

We identified a total of 1,110 suggestive loci for POAG ($p \leq 2.8 \times 10^{-4}$) from the mega-analysis (Table S1), of which 46 reached genome-wide significance as shown in Table 1. Only 2 of the 46 significant loci were previously reported in other glaucoma studies, as shown in the overlap of the Venn diagram in Figure S2A. Conditional analyses using Genome-wide Complex Trait Analysis-Conditional and Joint Association Analysis (GCTA-COJO)[44,45] identified 47 conditionally independent associations exceeding genome-wide significance ($p \leq 5 \times 10^{-8}$) (Table S2). All known and previously undescribed genes for POAG risk are annotated in Figure 2, with a full breakdown given in the Figure360 video. The quantile-quantile (QQ)-plot for this analysis is shown in Figure S2C.

We also replicated 37 (21%) of 174 previously reported POAG loci (listed in Table S3) at a Bonferroni-corrected significance for 174 loci (0.05/174; $p \leq 2.8 \times 10^{-4}$). Among these replicated associations are variants mapping to genes such as *ARHGEF12*, *CDKN2B-AS1*, *TMCO1*, *AFAP1*, *LMX1B*, and many more. Of note, rs9992186 (chr4: 46875929), mapping nearest to the *APBB2* gene, is in high linkage disequilibrium with rs59892895 ($R^2 = 0.81$), which has previously been associated with POAG risk in African ancestry individuals.[37] In our study, this association was also identified at suggestive GWAS significance (p value = 2.15×10^{-6}, odds ratio [OR] = 1.03), as reported in Table S1.

One of the previously undiscovered associations identified in the mega-analysis was the variant rs34957764, which maps to the Rho-associated coiled-coil-containing protein kinase 1 pseudogene 1 (*ROCK1P1*) gene region. Rho-associated coiled-coil kinase, a pseudogene resulting from partial duplication of the *ROCK1* gene, regulates cellular responses such as cell growth, proliferation, and apoptosis. We also identified a previously undescribed

variant (rs4938802) and known variant (rs11824032) that map to the *ARHGEF12* gene; the rs4938802 variant has previously been associated with elevated IOP and POAG risk in European ancestry individuals.[46,47] However, the previously undiscovered locus reported in our mega-analysis is in a different 250-kb region than the locus reported in the previous GWAS. Another previously undescribed variant of interest is rs145914721, mapping near to the *ADAMTS17* gene, which encodes a member of the ADAMTS protein family. Mutations in this gene, along with *ADAMTS10* and *LTBP2*, are associated with Weill-Marchesani-like syndrome, an inherited connective tissue disease characterized by lens abnormalities and secondary glaucoma.[48,49] Another previously undescribed variant, rs6462562, maps to the *SDK1* gene, which encodes for an adhesion molecule expressed in the cells that are damaged in POAG, retinal ganglion cells (RGCs), and in a subset of interneurons. This variant also promotes synaptic connectivity.[50]

Differential effects by sex

We conducted a sex-stratified GWAS in the discovery mega-analysis dataset (Figure S2B) and then meta-analyzed the sex-stratified results to differential effects by sex. We found 37 loci that reached the genome-wide significance threshold ($p \leq 5.0 \times 10^{-8}$). (Figure 2 green panel; Table S4.) Filtering for heterogeneity p value < 0.01 resulted in nine variants corresponding to three loci that showed evidence of heterogeneity between males and females. All nine variants in these three loci demonstrated a stronger effect in females (OR ranging from 1.87 to 1.92) than in males (OR ranging from 1.16 to 1.46, with lowest heterogeneity p value for rs1181192 at p = 0.0009). When calculating a Pearson correlation among effect sizes for all variants at p value < 0.01 in males and females, we observed a significant and strong correlation of 0.74 ($p < 0.0001$). This finding indicates a consistent pattern of genetic effects across sexes, suggesting minimal influence of sex-specific effects. Moreover, the relatively equal sample sizes in males and females further support the robustness and reproducibility of these associations within our study cohort.

Quantitative trait co-localization analyses

We examined the genetic co-localization[51] between SNPs identified from the discovery mega-analysis and SNPs identified in a GWAS of POAG endophenotypes from the POAAGG study.[38] These endophenotypes included IOP, cup-to-disc ratio (CDR), mean deviation (MD) from visual fields, and retinal nerve fiber layer (RNFL) thickness. Lead variant rs11824032 (chr11: 120354080) mapped to the *ARHGEF12* gene (PP4 > 0.8). In the included gene region, there were 2,091 variants considered in the co-localization analyses between POAG and baseline CDR (Table S5). The locus zoom plot for the *ARHGEF12* region's GWAS results is shown in Figure S2F. Further, we performed locus quantification to visualize the change in baseline CDR measurements with respect to the genotypes (Figure 3). Lastly, we conducted a follow-up two sample Mendelian randomization (MR) analysis at rs11824032 with baseline CDR as the exposure and POAG as the outcome, which resulted in a significant p value = 1.33×10^{-9} (beta = 12.02, SE = 1.98).

Replication of POAG associations in African ancestry datasets and meta-analysis

We performed replication analyses for the 47 risk loci (353 variants found in most of the replication datasets) identified in the conditional analyses in the discovery dataset in African

ancestry individuals extracted from four independent datasets (AOU, GGLAD-2, PMBB, and MVP). Two variants, mapping to the DBF4 zinc-finger pseudogene 2 (*DBF4P2*) and *ROCK1P1* genes and validated in independent datasets, were found to have a significant p value below the Bonferroni correction threshold (0.001) of 0.05/47 (Figure 4; Table S6). Locus zoom plots for these replicating genes are shown in Figures S2D and S2E. Variant rs34957764 mapping to the *ROCK1P1* locus on chromosome 18 reached the Bonferroni significant p value in the AOU dataset (p value = 0.0002) and showed a strong association with POAG in a meta-analysis of datasets (discovery p value = 4.93×10^{-24} and pooled meta p value = 1.67×10^{-24}). Variant rs1666698 mapping to the *DBF4P2* gene was marginally significant in the MVP dataset (p value = 0.0009, discovery p value = 3.59×10^{-10}, and pooled meta p value = 1.12×10^{-10}). Both replicated SNPs showed consistent effect direction across replication datasets.

We evaluated the minor allele frequency (MAF) of the two replicating variants (rs1666698 and rs34957764) in our study across multiple datasets. In addition to the discovery and replication datasets, we assessed the MAF in the 1000 Genomes populations, providing a comprehensive analysis of global allele frequencies. Figure S3 presents the MAF patterns of the two SNPs in the 1000 Genomes populations and the specific MAF values observed in each population within the discovery mega-analysis and replication datasets. rs1666698 exhibited consistent MAF across African populations, with MAF values exceeding 0.4. However, in European and East Asian populations, the MAF was much lower, approximately 1%. This stark difference in allele frequencies between African and non-African populations highlights the population-specific nature of this variant. rs34957764 displayed a distinct MAF pattern, with a prevalence of 20% in African populations compared with an MAF of 0.12 in other populations. This marked discrepancy in MAF between African and non-African populations underscores the significant population stratification and genetic diversity observed for this variant. This examination of MAF distribution offers valuable insights into the frequency and distribution of these variants across diverse populations, enhancing our understanding of their relevance in a global context.

Cross-ancestry comparisons

We compared the per-allele effect sizes and MAF between both previously known and undiscovered loci in our dataset of African ancestry individuals (Figure S4A). Previously undiscovered variants identified from the mega-analysis have large effect sizes in African ancestry individuals, whereas previously known variants from non-African populations (i.e., GBMI GWAS on POAG) show smaller effect sizes. We also calculated the genetic impact correlation (ρ_{gi}) using Popcorn,[52] which is the correlation coefficient of the population-specific allele-variance-normalized SNP effect sizes (Figure S1C). Genetic correlations between ancestries ranged from $\rho_{gi} = 0.59$ (African with East Asian ancestry) to $\rho_{gi} = 0.73$ (African with European ancestry), with the highest correlation among East Asian and European ancestry individuals ($\rho_{gi} = 0.78$).

Since the majority of large GWAS for POAG have been performed in non-African ancestry individuals, we next demonstrated the added value of including African ancestry individuals

when explaining phenotypic variability for POAG (Figure S4B). GCTA-restricted maximum likelihood (REML) analyses[53] showed that the estimate of variance for POAG was 0.0295 (SE = 0.006) for previously known loci but increased to 0.05 when including both previously known loci and undiscovered loci from our mega-analysis (Figure S4B). Of note, the previously undiscovered variants from our mega-analysis explained 0.041 variance, so the highest estimate of variance (after suggestive significant hits) came from the inclusion of both previously known and undiscovered loci from our African ancestry cohort.

Prioritizing causal variants, genes, and pathways

Functionally informed fine-mapping—Combining annotations using fine-mapping approaches has been proven to enhance the ability to localize causal variants. Using integrated regulatory annotations from epigenome integration across multiple annotation project (EpIMAP),[54] we prioritized putative causal variants identified through our discovery mega-analysis.[55] We performed fine-mapping using SuSIE[56] (STAR Methods), which uses functional enrichment of regulatory regions to weight the GWAS summary statistics and compute a posterior probability. This analysis identified 51 credible set pairs with posterior probability >95% for containing a causal variant. There were four variants that mapped to enhancer regions among the credible sets: rs371063473 (*LOC101929650*), rs4809477 (*SLCO4A1*), rs73719555 (*LOC285766*), and rs73669125 (*LMX1B*) (Table S7). Of note, the rs73669125 variant is nearest to the *LMX1B* gene; this gene is known to be involved in the development of the anterior segment of the eye.[57] Additionally, a mutation in *LMX1B* is known to cause nail-patella syndrome (NPS), an inherited developmental disorder; one of the manifestations of NPS includes the development of open-angle glaucoma.[58–63] The rs73235527 variant maps to the gene *BEND4*; this gene is associated with retinitis pigmentosa 26.[64]

In our investigation of potential biological insights from the mega-analysis summary statistics, we conducted pathway analyses using the multivariate analysis of genomic annotation (MAGMA) tool, which is seamlessly integrated within the functional mapping and annotation (FUMA) platform.[65,66] The MAGMA gene set pathway analysis allowed us to explore the enrichment of curated gene sets and Gene Ontology (GO) terms sourced from MsigDB.[67] Following the MAGMA analyses and correction for multiple testing using the Bonferroni method, we identified three pathways that exhibited significant enrichment at a corrected p value threshold (p_{bon}) < 0.05. The specific enriched pathways include negative regulation of translation in response to stress (p = 5.14–08), cellular response to leucine starvation (p = 6.52–08), and negative regulation of CREB transcription factor activity (p = 3.52–07).

Quantitative expression of POAG-associated genes in human eye tissues —The pathogenesis of POAG involves the loss of RGCs and damage to trabecular meshwork (TM) cells, which can be caused by increased oxidative stress.[68] We induced oxidative stress with H_2O_2 in human ocular cell lines to understand gene expression patterns and to determine this stressor's functional relevance in POAG. We quantified the expression profiles of the nearest genes to the three likely causal variants from the mega-analysis in human TM (hTM) cells and RGCs derived from induced pluripotent

stem cells (iPSC-RGCs)[69] treated with H_2O_2. We include a video that demonstrates the electrophysiological responses of iPSC-RGCs in cell culture at day 71 obtained using patch-clamp recording in a whole-cell configuration mode (Video S1). These variants included the two loci demonstrating replication in independent African datasets (rs34957764 mapping to *ROCK1P1* and rs1666698 mapping to *DBF4P2*) and the loci associated with baseline CDR in genetic co-localization analyses (rs11824032 mapping to *ARHGEF12*). Gene expression in human retinal tissues from normal and glaucoma donors was also quantified for these three nearest genes.

When comparing hTMs under oxidative stress to untreated hTMs, we found significant overexpression of *ARHGEF12* (30.2 ± 1.05, p value = 0.008). *ROCK1P1* was marginally increased (2.2 ± 0.5), while no expression of *DBF4P2* was detected (Figure 5A). In stressed versus untreated iPSC-RGCs, the *ROCK1P1* (2.45 ± 0.45, p value = 0.009) and *DBF4P2* (2.15 ± 0.4, p value = 0.02) genes were significantly upregulated. There was an upward trend in the expression of *ARHGEF12* (1.6 ± 0.4) (Figure 5B). With respect to human retinal tissue samples, there was no significant difference in the expression of *ARHGEF12* (11.4 ± 4.05) and *ROCK1P1* (17.4 ± 3.8) in the retinal tissue isolated from a POAG patient compared with the normal retinal tissue sample; however, *DBF4P2* (198 ± 0.3, p value: 0.0003) was significantly upregulated in the retinal tissue from the POAG patient (Figure 5C). The possible mechanisms involving the variants in the *ARHGEF12* and *ROCK1P1* genes and their relation to POAG are shown in Figure 5D.

In silico analysis of gene expression in ocular tissues

We assessed the expression levels for the genes that are nearest to the loci that replicated in independent African ancestry datasets (*ROCK1P1* and *DBF4P1*) and were associated with baseline CDR in genetic co-localization analyses *in silico* (*ARHGEF12*), wherever data were available. We used the most current publicly available source, the Human Eye Transcriptome Atlas (HETA).[70,71] This database contains the largest number of distinct ocular tissues, compared with all earlier databases, and it is the only database employing fresh rather than postmortem tissue for transcriptome analysis, a clear advantage for accuracy of results. As there is no ocular tissue information in Genotype-Tissue Expression (GTEx)[72] or Encyclopedia of DNA Elements (ENCODE)[73] databases, we did not utilize these for determining gene expression.

ARHGEF12 is widely expressed in ocular tissues, including the ON. *ROCK1P1* is expressed in the ON and in the peripheral retina but not in the retinal center. These findings are consistent with the location of RGCs and their axons. The transcriptional profile of *DBF4P2* is not available. The only transcriptional profile available is for *DBF4P1* and this would have uncertain relevance to the gene of interest.

Polygenic prediction of POAG in African ancestry

Summary statistics from the discovery mega-analysis (African ancestry individuals) were used to create a PRS_{MEGA}, and summary statistics from GBMI (European ancestry individuals) were used to create a PRS_{GBMI}. Each PRS was calculated using PRS-CS and was applied to three independent datasets of African ancestry individuals (eMERGE, n =

13,493; GGLAD-2, n = 1,490; PMBB, n = 11,117), and the AUC was compared (Table S8). The highest AUC was achieved in the GGLAD-2 data (AUC = 0.657) with summary statistics from the mega-analysis. We also compared individuals identified in the top 20% of the PRS by both mega-analysis and GBMI reference data and the remainder of the dataset. The PRS_{MEGA} outperforms the PRS_{GBMI} in two out of the three datasets, as shown in Figure 6 and Table S8.

DISCUSSION

Only two percent of genetic studies have focused on individuals of African ancestry as of 2019.[74] Even diseases that disproportionately affect African ancestry individuals, such as POAG, remain understudied in this population. To help address this disparity, we conducted a very large GWAS on POAG in African ancestry individuals to date (n = 11,275). We identified 46 risk loci at genome-wide significance in our discovery cohort. Two of these loci, mapping to the *ROCK1P1* and *DBF4P2* genes, replicate in independent African ancestry datasets, and one previously undescribed locus mapping to the *ARHGEF12* gene is associated with baseline CDR in genetic co-localization analyses. We show through subsequent functional analyses that these three loci can be logically implicated in African ancestry POAG pathogenesis.

This mega-analysis of African ancestry individuals enables the identification of previously undescribed risk loci for POAG, while also replicating risk loci across ancestries. The majority of previously associated loci identified in other ancestral populations do not replicate at a conventional genome-wide significance level, possibly due to genetic heterogeneity across different ancestry groups. However, 21% replicate at the Bonferroni threshold p value for 174 previously reported unique loci.

Significant findings from the discovery mega-analysis replicate in four independent datasets of African ancestry, chosen due to their use of the same imputation panel as our study (with the exception of AOU, which consists of whole-genome sequence data). Two loci from the discovery mega-analysis replicate within these African ancestry datasets. The rs34957764 variant mapping to the *ROCK1P1* locus replicates in the AOU dataset, and the rs1666698 variant mapping to the *DBF4P2* gene replicates in the MVP dataset and in meta-analyses of all replicated datasets (p value = 0.002); both replicated SNPs also showed consistent effect estimates in most replication datasets. The observed MAF differences between African and non-African populations for rs1666698 and rs34957764 highlight the influence of population-specific genetic factors in shaping allele frequencies. The substantial variation in MAF suggests potential differences in the evolutionary history and selective pressures experienced by these populations. These findings support the importance of considering population-specific effects when investigating the functional and clinical implications of genetic variants. Furthermore, the contrasting MAF patterns underscore the need for careful interpretation of genetic association studies conducted in diverse populations. The substantial differences in MAF for these two variants between African and non-African populations may have implications for disease risk assessment, drug response, and population-specific genetic studies.

ROCK1P1 and *DBF4P2* are both pseudogenes. *ROCK1P1* is located on chromosome 18p11.32 and is a result of the partial duplication of the *ROCK1* gene on chromosome 18q11.1. ROCK1 is a serine/threonine kinase and a downstream effector of the Rho GTPase. ROCK1 is a target for Rho kinase inhibitors to reduce aqueous humor outflow resistance by directly acting on TM cells and Schlemm's canal. These inhibitors are used as a treatment for glaucoma.[75–77] Despite a lack of clear evidence on the strength of the underlying mechanisms, our analysis highlights the potential importance of these sites. The MAF of rs34957764 is 0.25 in African ancestry samples, compared with 0.12 in European ancestry samples. By contrast, the MAF of rs1666698 is substantially higher in African and African American populations (MAF = 0.4) than in Europeans (MAF = 0.02). These findings underscore the need for additional studies to elucidate the functional significance of these SNPs and their potential contribution to disease susceptibility in diverse populations.

We also identify genetic co-localization between a lead variant mapping to *ARHGEF12* and baseline CDR. The *ARHGEF12* gene has previously been associated with elevated IOP in individuals of European ancestry.[46] The genetic co-localization between rs11824032 and baseline CDR is not previously reported. Although the significant MR p value provides supporting evidence for a potential causal association, we acknowledge the limitations of interpreting causality based on a single-SNP MR test. It is important to consider the complexities of establishing directionality in such analyses. Furthermore, we acknowledge that the observed association between rs11824032 and baseline CDR may be influenced by other factors specific to this ancestry group. For example, individuals in this group may experience earlier and more severe neurodegeneration compared with less affected ancestry groups, which could also contribute to the observed association.

Our quantitative real-time PCR data indicate that *ROCK1P1* mRNA is significantly overexpressed in iPSC-RGCs under oxidative stressed conditions. *In silico* analysis demonstrates that *ROCK1P1* is expressed in the ON and peripheral retina, consistent with the location of RGCs and their axons. *ARHGEF12* is overexpressed in hTM cells under stressed conditions and shows a trend toward overexpression in iPSC-RGCs but fails to reach significance. *In silico* analysis confirms that *ARHGEF12* is expressed in the ON. There are also upward trends detected in the expression of the *ARHGEF12* and *ROCK1P1* genes in the retinal tissue isolated from a POAG patient, but these expression profiles are not statistically different when compared with control retina. The retina is comprised many different layers, and it is possible that the full retinal biopsy obscures the expression of genes located in the RGC layer, which is most affected by glaucoma.

The *ARHGEF12* (Rho guanine nucleotide exchange factor [GEF] 12) gene is located on chromosome 11q23.3; an intronic variant rs58073046 in this gene has previously been associated with glaucoma and IOP.[46] ARHGEF12 is reported to function downstream of the RhoA/Rho-associated kinase pathway, which is known to regulate TM plasticity via actin-myosin interactions.[78–80] It is proposed that ARHGEF12 activates RhoA, which leads to ROCK activation, causing a decrease in aqueous humor outflow and permeability of Schlemm's canal cells.[81] The result is a subsequent increase in IOP, contributing to increased CDR in African ancestry populations. Additionally, the *ARHGEF12* gene interacts with ABCA1 and is reported to bind directly to the C terminus of ABCA1 to activate

RhoA. Simultaneously, ARHGEF12 prevents the degradation of ABCA1 by extending its half-life.[82,83] Variants in *ABCA1* have previously been found to be associated with both POAG and IOP.[84,85]

RhoA/ROCK and transforming growth factor (TGF)-β signaling pathways also play a significant role in the pathogenesis of POAG.[86–88] TGF-β2 is the predominant form of the three isoforms in the eye.[89,90] Analyses of the aqueous humor and TM cells from glaucoma patients have detected increased levels of TGF-β2,[91] causing high levels of ECM deposition in TM, ON head, and lamina cribrosa,[88,92] leading to the death of RGCs and atrophy of the ON. This mechanism can possibly explain the increase in CDR observed in our group of African ancestry individuals that carry the *ARHGEF12* and *ROCK1P1* variants.

This study demonstrates that the inclusion of African ancestry individuals in several analyses improves the prediction of POAG risk for these individuals. First, a comparison of per-allele effect sizes demonstrates that previously undiscovered variants from the mega-analysis have large effect sizes in African ancestry individuals, whereas previously reported variants (mainly from European individuals) tend to have smaller effect sizes that point to the polygenic tail of POAG risk.[93] Additionally, in a cross-ancestry genetic correlation analysis, we demonstrate lower genetic correlation among African and East Asian individuals (59%) and African and European individuals (73%), compared with European and East Asian individuals (78%). It is certainly possible that the smaller effect sizes in our study are not due to differences in biology but rather to the Winner's Curse,[94] whereby the initial discovery (in Europeans) is an overestimate of the effect sizes. Additional studies should be conducted in large global populations to obtain more estimates of the effect size of these variants. We also show that the inclusion of both previously known and undiscovered loci from our African ancestry cohort helps to increase the estimate of variance for POAG from GCTA-REML analyses. Finally, we demonstrate that the PRS_{MEGA} (African ancestry) showed an improved prediction of disease risk over the PRS_{GBMI} (European ancestry) in two out of three African ancestry cohorts, despite the much smaller size of the PRS_{MEGA} dataset. Notably, the PRS_{MEGA} demonstrated an improved ability to discern individuals in the top 20^{th} percentile of PRS distribution, suggesting the clinical utility of the PRS in African ancestry individuals.

This study has several major strengths, beginning with the implementation of data integration strategies to combine genotype data from 11,275 African ancestry individuals into a megaanalysis dataset, allowing us to achieve substantial statistical power. Several previous studies have shown that mega-analyses combining individual-level data are superior to meta-analyses, which rely on summary statistics from numerous heterogeneous samples.[95,96] Our findings further support the existing literature, as we demonstrate a strong correlation ($r = 0.86$) between the mega-analysis and meta-analysis results. Moreover, our results suggest that the mega-analysis approach, which combines individual-level data, exhibits higher statistical power, particularly for detecting smaller-effect-sized variants. Although mega-analyses may not always be practical due to constraints such as data availability and other logistical challenges, our study was fortunate to have comprehensive individual-level data across multiple datasets. This approach allows us to pool the row-level data, thereby increasing the statistical power of our analysis and facilitating more

precise estimates of the effects under investigation. Another strength of our study is that the POAAGG study carefully ascertained quantitative phenotypic traits from each subject, which is crucial to prevent residual confounding effects of unmeasured phenotypes within association studies. This rich dataset allows us to study and identify significant differences in quantitative trait measurements for genotypes from our mega-analyses in a case-only analysis. Finally, we employ multi-factorial strategies to improve the detection of potential causal variants, genes, and biological pathways that contribute to POAG pathophysiology. By incorporating functionally informed fine-mapping methods, co-localization of GWAS signals from binary and quantitative phenotypes, and *in silico* validation methods, we are able to prioritize variants and systemically characterize genes in pathways to elucidate POAG mechanisms.

In conclusion, this study greatly expands our knowledge of the genetic landscape of POAG in African ancestry individuals. Though the increased burden of POAG in this ancestry group was identified more than three decades ago, new generations continue to experience premature vision loss from this familial disease. A critical barrier to progress has been the lack of genetic studies of POAG in African ancestry individuals. Genetic studies are needed to identify novel targets for screening and therapeutic intervention, as all treatment options target only one disease mechanism, elevated IOP, with limited success.[97] This study represents a crucial first step toward addressing this disparity by conducting the largest-ever GWAS on POAG in African ancestry individuals. Although more experimental evidence is ultimately required to pinpoint causal mechanisms and generate predictive tools for early screening of POAG, many useful insights can be drawn from our study. Our work is an important step toward achieving future goals, including defining subgroups of disease that aid in early detection, providing the capability for early screening within families, and discovering targetable pathways for personalized therapeutic interventions. Future studies can also help to determine whether African ancestry individuals have different responses to treatments, such as recently approved ROCK inhibitors. POAG is the leading cause of irreversible blindness in the world today, and familial blindness perpetuates increased morbidity, poverty, and mortality across generations. The lack of genetic studies in the most affected African ancestry population is both a failure of science and a failure of our moral obligation to address systemic racism prevalently visible today.

Limitations of the study

A limitation of this study is the relatively small sample size of our African ancestry discovery cohort. Although this may be the largest African ancestry GWAS for POAG to date, it is still smaller than many GWAS in datasets of European ancestry individuals. Nevertheless, the African ancestry PRS_{MEGA} for POAG risk stratification still shows improvement over European ancestry PRS_{GBMI}, which was drawn from a much larger dataset (GBMI). Recruiting more individuals of African ancestry should be a priority for developing a more refined PRS with clinical utility for POAG diagnosis in African ancestry populations; this is imperative because 50% of patients with POAG are unaware that they are afflicted with this blinding disease. A second limitation of the study is posed by the remarkable diversity of African ancestry populations, which are more dissimilar than any other ancestry group worldwide.[98] This diversity could provide one reason for lack of

replication of many loci in our replication datasets. Additionally, many of the replication datasets relied on diagnosis code-based case/control definitions for POAG, which could also be responsible for the lack of replication of many signals. These datasets were also characterized by imbalanced case/control ratios, which may introduce some degree of uncertainty or misclassification. Although we estimate effect sizes in these independent replication datasets and perform meta-analyses to enhance robustness, it remains essential to interpret the observed effect sizes with caution, due to the potential impact of these limitations on the precision and accuracy of results. Another possible limitation of our study is the potential impact of study source as a confounding factor. Although we followed the imputation strategy shown to be robust in previous studies,[99,100] study source can still represent a potential source of bias.[96] However, it is worth noting that in these analyses, using study source as a covariate was challenging due to the uneven distribution of cases and controls among the three datasets in the discovery analyses. Although the GGLAD and POAAGG datasets have fairly equal divisions between cases and controls, the ADAGES study has a very high distribution of cases (92%), which can cause the ADAGES batch to be highly correlated with case status. This would result in multicollinearity issues in the sensitivity analyses. We also do not believe that including the study source as a covariate in sensitivity analyses would substantially alter our main findings. Nonetheless, we acknowledge the potential impact of the study source on our results and have taken steps to account for potential confounding factors through estimating the inflation factor and performing conditional analyses and replication analyses. We performed sensitivity analyses that compare the results of meta-analyses of the discovery datasets and mega-analyses, providing additional insights into the robustness of our findings. Finally, although we used today's industry-standard analyses for imputation, GWAS analysis, and PRS analysis, it will be important to continue to develop new methodologies that incorporate local ancestry into the analyses, which we anticipate will further improve the identification of both ancestry-specific association signals as well as those that are relevant across multiple ancestry groups.

STAR★METHODS

RESOURCE AVAILABILITY

Lead contact—Further information and requests for resources and reagents should be directed to and will be fulfilled by the lead contact, Joan O'Brien (joan.o'brien@pennmedicine.upenn.edu).

Materials availability—This study did not generate new unique reagents.

Data and code availability

- Genotype data for POAAGG and ADAGES study participants have been deposited in the database of Genotypes and Phenotypes (dbGaP) and are publicly available as of the date of publication. Genotype data for GGLAD study participants are publicly available through the link listed in the key resources table. This paper also analyzes existing publicly available data from All of Us, eMERGE Phase III, and Global Biobank Meta-Analysis Initiative (GBMI). The accession numbers for these datasets are listed in the key resources table. Penn

Medicine BioBank (PMBB) and Million Veteran Program (MVP) data can be accessed via collaborations with researchers upon request. Raw data from the quantitative gene expression data from Figure 5 is uploaded to Mendeley Data: https://doi.org/10.17632/7drg5smn9j.1.

- This paper does not report original code.
- Any additional information required to reanalyze the data reported in this paper is available from the lead contact upon request.

EXPERIMENTAL MODEL AND STUDY PARTICIPANT DETAILS

Human Participants—This study included three African ancestry datasets in the discovery analyses (n=11,275): (1) African Descent and Glaucoma Evaluation Study study (n=1,999), (2) Genetics of Glaucoma in People of African Descent consortium (n=2,952), and (3) Primary Open-Angle African American Glaucoma Genetics study (n=6,324). Replication was performed in four African ancestry datasets: (1) a second dataset from GGLAD (referred to as GGLAD-2; n=1,492), (2) All of Us (n=22,914), (3) Penn Medicine BioBank (n=9,512), and (4) Million Veteran Program (n=9,586). Detailed information on the recruitment and phenotyping of participants is included in Figure 1. The study adhered to the tenets of the Declaration of Helsinki and was approved by the University of Pennsylvania Institutional Review Board. All subjects provided informed written consent under IRB-approved protocols.

Cells Lines—The eye tissues for our study were isolated from two pairs of eyes collected from non-diabetic European ancestry donors who registered voluntarily to donate to the eye bank. One eye pair was collected from a 91-year female donor with a clinical history of glaucoma managed using Brimonidine (Alphagan®) eye drops, and the second eye pair was collected from a 91-year-old female with no history of glaucoma. Informed consent about the tissue use for research was obtained from donors, with a death-to-preservation interval of <6 hours. Both eyes were collected and processed by the Lions Eye Institute of Transplant and Research recovery personnel and were preserved in RNA-later (Qiagen, Valencia, CA, USA) for the left eye, and 2% glutaraldehyde and 1% paraformaldehyde in 0.1 M phosphate buffer for the right eye. The left eyes were shipped overnight on wet ice to the University of Pennsylvania and were processed upon arrival. The normal or glaucoma status of donor's right eyes was assessed for the stage of glaucoma by staining longitudinal sections of the ON area using hematoxylin and eosin and evaluated for bowing of lamina cribrosa, ON cupping, widening of arachanoid space, and characteristic thinning of RGC layer. The left eyes, preserved in RNA-later solution, were examined by photography with a stereomicroscope before dissection. For each donor's eye, ocular tissues from eye globes were carefully collected to minimize sample contamination.

The primary trabecular meshwork cells were commercially obtained from Sciencell, CA, USA (Cat#6590) and also as a gift from Dr. Markus Kuehn, University of Iowa. We validated the authenticity of the TM cells by performing MYOC induction experiments with dexamethasone, as described previously.[108] We used Passage 2 (P2) to Passage 4 (P4) primary TM cultures for all our experiments.

The iPSCs were isolated and differentiated from the PBMCs of a 41-year-old African American male. The iPSC-RGCs for our studies were derived using small molecules to inhibit BMP, TGF-beta (SMAD), and Wnt signaling to differentiate iPSCs into RGCs. The generation and characterization of these cells are previously described.[69,109,110]

The University of Pennsylvania and Children's Hospital of Philadelphia Human Subjects Research Institutional Review Board approved all human sample collection protocols following the Declaration of Helsinki. Written informed consent was obtained from the human cell donor.

METHOD DETAILS

Study Design and Participants—For the discovery analyses, we obtained data on 6,003 POAG cases and 5,272 controls of African ancestry from three independent cohorts across the world. In brief, the POAAGG study population consists of self-identified Blacks (African American, African descent, or African Caribbean), aged 35 years or older, recruited from the Philadelphia area. In both the ADAGES study and the GGLAD consortium, subjects self-identified as having African ancestry. Previously published case/control definitions were used for all studies.[36,37,111] Among the GGLAD and ADAGES data, we only included individuals with age and sex information. Individuals with missing age and sex were excluded from the analyses during quality control checks.

We imputed each dataset using the TOPMED imputation reference panel[39] and then merged all three TOPMED imputed datasets into one larger dataset to perform a mega-analysis of African ancestry participants.[99]

For the replication analyses, we analyzed four independent datasets (GGLAD-2, All of Us, Penn Medicine BioBank, and Million Veteran Program) (Table 1). For the GGLAD-2 dataset, we used age- and sex-matched participants from the previous GGLAD study that were excluded from the discovery analyses due to the absence of covariates. For all replication datasets, only African ancestry individuals were included.

Quality Control and Imputation—We imputed the POAAGG, GGLAD and ADAGES data to the TOPMED reference panel[39] and merged the three datasets using BCFtools to preserve the dosage information in the VCF files. We then performed post-imputation quality control by filtering SNPs with average imputation R^2<0.3, MAF <1%, and/or evidence of significant deviation from Hardy-Weinberg Equilibrium (p-value<1e-08). We performed Principal Component Analyses (PCA) on the merged dataset using the EIGENSOFT package where the PCs are projected on to the 1000 Genomes dataset.[101,102] The scree plots demonstrate the proportion of variance explained by each of the 20 PCs in the merged POAAGG dataset. Since the elbow is at PC6, we included the first 6 PCs in all subsequent association analyses to control for population stratification.

Discovery Mega-Analysis—Association testing for the discovery mega-analyses was performed assuming an additive model in which the imputed genetic dosages for each variant were tested against the case-control status, using SAIGE version 1.1 software.[103] This applies a mixed linear approach to association testing while accounting for cryptic

relatedness in the population. All variants at MAC>20 were evaluated using firth regression in SAIGE. All models were adjusted for age and the first 6 PCs in the mega-analyses. Three mega-analyses were performed on 11,275 individuals (6,003 cases and 5,271 controls). Plots were created in R (Version 3.6.3) and python and regional plots were created using LocusZoom web interface.[104] We calculated the genomic inflation factor for each analysis to ensure that the results were not inflated due to population substructure, cryptic relatedness, or model misspecification using LDSC software.[105,106] We used the PLINK LD clumping method to identify the number of independent risk loci. This was achieved by clumping variants (p-value<5e-08) within 500kb regions and r^2>0.001 into a single locus. Additionally, for regions where multiple variants in high linkage disequilibrium mapped to multiple genes, we conducted conditional analyses for each variant in the region to identify the number of independent loci using GCTA-COJO software using default parameters.[45]

Sensitivity Analyses—We compared the results obtained from the mega-analysis with a meta-analysis of the three datasets (POAAGG, GGLAD and ADAGES) by conducting correlation analyses. We calculated the Pearson correlation coefficient to assess the agreement between the two approaches. Additionally, we generated Figure S1 to visually compare the absolute betas obtained from mega-analysis and meta-analysis.

Identifying Known Risk Loci and Associations—To identify genomic regions that were previously known to be associated with POAG through numerous studies, we used the NHGRI-EBI GWAS catalog[43] to download all previously published POAG loci (download date: 12/17/2022). We clumped all SNPs into independent risk loci. We then looked at SNPs identified by our discovery mega-analysis in this list by searching for LD friends via the GCTA package.[44] GCTA uses regression approach to search for SNPs that are in significant LD with the provided list. We identified all SNPs that are in LD with known SNPs in 10KB upstream and downstream region of the known risk loci regions.

Sex-Stratified Analysis—We performed a sex-specific GWAS in our mega-analysis dataset by stratifying 6,498 females-only, and 4,776 males-only. The analyses were conducted following the same plan as the full discovery mega-analysis using the SAIGE mixed linear model and adjusting single variant analyses by age and first 6 principal components. To identify variants that are differentiated by sex, we meta-analyzed the sex-stratified GWAS using PLINK and considered genome-wide significant variants with heterogeneity P-value <0.01. Among these significant variants, we then applied 500kb and r^2>0.1 LD clumping threshold to identify significant sex differentiated POAG loci.

Trait Co-localization Analysis—At each significant locus identified using PLINK clumping methods, we performed a co-localization analysis between our discovery mega-analysis and a GWAS of POAG endophenotypes from the POAAGG study (IOP, CDR, MD from visual fields, and RNFL thickness) using coloc package in R.[112,113] For the traits that demonstrated significant co-localization, we extracted all variants that were in high LD with independent loci (500 kb r^2>0.5) to look for correlation of betas among all SNPs. We reported the colocalized signals for variants that were significantly different from 0. Next, we identified loci that demonstrated posterior probability for H4 >0.8 and

conducted a two sample Mendelian randomization analysis (Wald ratio test) to identify the causal relationship of the variant between case/control POAG status and each quantitative trait, where quantitative trait is exposure and POAG binary variable as outcome. We used eQTpLot[114] for further locus quantification and visualization of the signals with PP4>0.8.

Replication and Joint Meta-Analysis—We performed a single variant association test in all 353 genome-wide significant variants (46 loci) in all replication datasets using PLINK dosage analyses. Variants that reached below a loci-based Bonferroni threshold (p-value=0.05/46 =0.001) in any of the replication datasets were then meta-analyzed with the discovery dataset using Forest PM package.[115] Forest plots for the replicated loci were generated using the Forest PM package and the random effects meta-analyses p-values were reported for each replicated signal.

Heritability Estimation—LD scores were calculated on all samples from the mega-analyses using LDSC software.[105,106] We choose a default window size of 1cM to calculate LD scores. We partitioned SNP-based heritability using stratified LD score regression by the same functional annotation categories as used in fine-mapping using LDSC software.[105] We calculated enrichment scores in each category as the proportion of SNP heritability in the specified category, divided by the proportion of total SNPs annotated to that category. The p-value was determined through a two-tailed test to identify the categories that have an enrichment score >1.

Cross-Ancestry Comparison—For cross ancestry comparison, we used summary statistics from a recent POAG GWAS from GBMI,[17,116] which includes GWAS summary statistics from a European ancestry GWAS, East Asian ancestry GWAS, and multi-ancestry GWAS (contains approximately 10% African ancestry individuals). A total of 5,257,495 variants from our discovery mega-analyses were found in GBMI summary statistics. After aligning effect alleles, we compared effect estimates and minor allele frequencies using Pearson's correlation coefficient. We used Popcorn (version 1.0)[52] to estimate the per-allele genetic impact correlation coefficient (ρ_{gi}) between the discovery mega-analysis and GBMI European and East Asian meta-analyses, respectively. The LD reference panel for Popcorn was generated using the 1000 Genomes Phase 3 dataset,[117] consisting of Hapmap3 variants only for AFR, EUR, and EAS populations as defined by 1000 Genomes.

Functionally Informed Fine-Mapping—We used the implementation of SuSie in PolyFun (POLYgenic FUNctionally informed fine-mapping)[56] to perform fine-mapping of 257 SNPs (p-value $<1x10^{-05}$) in overall mega-analyses results. The variants were mapped to the nearest gene and annotated to regulatory regions from the EpiMap database.[54] We allowed for the presence of 10 causal SNPs per locus, as per the recommendations from PolyFun.[56] We identified causal variants by filtering the results with posterior probabilities (PIP) >0.9.

Pathway Analyses—In this study, we conducted pathway analyses to uncover potential biological insights from genome-wide association studies (GWAS) mega summary statistics. To achieve this, we utilized MAGMA (Multivariate Analysis of Genomic Annotation), a powerful tool for pathway analysis, integrated within FUMA (Functional Mapping

and Annotation).[65] MAGMA gene-set analysis[66] is conducted for curated gene sets and GO terms obtained from MsigDB.[67] To account for multiple testing, which arises from the analysis of numerous pathways, we applied Bonferroni correction. These corrections ensured stringent control of the type-I error rate and increased the confidence in identifying significantly enriched pathways. GO pathways with $P_{bon} < 0.05$ were considered significant.

Evaluating Oxidative Stress in TM cells and iPSC-RGCs—The primary TM cells and iPSC-RGCs were incubated with increased amounts of H_2O_2 overnight before replacing the cultures with complete media. The cells were collected 24 hours after the H_2O_2 treatment, and levels of selected gene transcripts were determined using quantitative RT-PCR and gene expression primers, following published protocols.[118–120] The relative gene expression was compared against control (no treatment) to obtain normalized gene expression. Expression levels (±SEM) were calculated by analyzing in triplicate reactions and presented on an arbitrary scale that represents the expression of relevant genes compared to the housekeeping gene *GAPDH*. An increase in *Superoxide Dismutase 1* (*SOD1*) expression levels served as a positive control for oxidative stress in the same set of samples. A limitation of using this approach as a stressor is that it does not recapitulate a disease relevant process.

***In Silico* Analyses for Gene Function—**We evaluated the expression of genes that contained likely causal loci in human ocular tissues using a publicly available database: The Human Eye Transcriptome Atlas.[70,71] This Atlas consists of gene expression data from healthy and diseased human eye tissues. The gene expression is derived from 100 surgical samples from 15 different ocular tissues collected at the Eye Center at the University of Freiburg. To ensure accuracy of expression data, findings were normalized across all 100 specimens. Previously defined tissue specific biomarkers were used to perform deconvolution using xCell. Clustering by tissue type was established with high tissue specificity. In contrast to all other ocular transcriptome data bases, no human donor eyes were included in this dataset. This improved accuracy for RNA-based findings.

Polygenic Risk Scores (PRS)—We use discovery mega-analysis summary statistics and GBMI summary statistics to generate two separate PRS for POAG: PRS_{MEGA} and PRS_{GBMI}. Each PRS was computed using PRS-CS[121] with 1KG African reference panel for the mega-analyses and 1KG European ancestry panel for the GBMI analyses. We validated each PRS in three independent[37,100,122] cohorts of African ancestry individuals (eMERGE, PMBB, and GGLAD-2 datasets). Descriptive statistics for these datasets are reported in Table 1. The prediction accuracy of the PRS_{MEGA} and PRS_{GBMI} was estimated by calculating the Nagelkerke R^2, which is the difference of R^2 between a full model including PRS and covariates (age, sex and principal components) and reduced model which only includes covariates.

QUANTIFICATION AND STATISTICAL ANALYSIS

For the quantitative gene expression data, all data are represented as mean + SEM. Each experiment was conducted in triplicates for statistical analysis. Differences in gene transcript expression between treatment groups were analyzed using Student T-test by statistical

software (GraphPad Prism 6.0; GraphPad Software, Inc., La Jolla, CA, USA). *p-values of < 0.05 were considered statistically significant.

Supplementary Material

Refer to Web version on PubMed Central for supplementary material.

Authors

Shefali S. Verma[1,29], Harini V. Gudiseva[2,29], Venkata R.M. Chavali[2], Rebecca J. Salowe[2], Yuki Bradford[3], Lindsay Guare[3], Anastasia Lucas[3], David W. Collins[2], Vrathasha Vrathasha[2], Rohini M. Nair[2], Sonika Rathi[2], Bingxin Zhao[4], Jie He[2], Roy Lee[2], Selam Zenebe-Gete[2], Anita S. Bowman[2], Caitlin P. McHugh[5], Michael C. Zody[5], Maxwell Pistilli[2], Naira Khachatryan[2], Ebenezer Daniel[2], Windell Murphy[6], Jeffrey Henderer[7], Regeneron Genetics Center[8], Tyler G. Kinzy[9,10], Sudha K. Iyengar[9,10], Neal S. Peachey[10,11],
VA Million Veteran Program,
Kent D. Taylor[12], Xiuqing Guo[12], Yii-Der Ida Chen[12], Linda Zangwill[13], Christopher Girkin[14], Radha Ayyagari[13], Jeffrey Liebmann[15], Chimd M. Chuka-Okosa[16], Susan E. Williams[17], Stephen Akafo[18], Donald L. Budenz[19], Olusola O. Olawoye[20], Michele Ramsay[21], Adeyinka Ashaye[20], Onoja M. Akpa[22], Tin Aung[23], Janey L. Wiggs[24], Ahmara G. Ross[2], Qi N. Cui[2], Victoria Addis[2], Amanda Lehman[2], Eydie Miller-Ellis[2], Prithvi S. Sankar[2], Scott M. Williams[25], Gui-shuang Ying[2], Jessica Cooke Bailey[9,10,28], Jerome I. Rotter[12], Robert Weinreb[13], Chiea Chuen Khor[26], Michael A. Hauser[27], Marylyn D. Ritchie[3,30], Joan M. O'Brien[2,30,31,*]

Affiliations

[1]Department of Pathology and Laboratory Medicine, Perelman School of Medicine, University of Pennsylvania, Philadelphia, PA, USA

[2]Scheie Eye Institute, Perelman School of Medicine, University of Pennsylvania, Philadelphia, PA, USA

[3]Department of Genetics, Perelman School of Medicine, University of Pennsylvania, Philadelphia, PA, USA

[4]Department of Statistics and Data Science, The Wharton School, University of Pennsylvania, Philadelphia, PA, USA

[5]New York Genome Center, New York, NY, USA

[6]Windell Murphy, MD, Philadelphia, PA, USA

[7]Department of Ophthalmology, Lewis Katz School of Medicine, Temple University, Philadelphia, PA, USA

[8]Tarrytown, NY, USA

[9]Department of Population and Quantitative Health Sciences, Cleveland Institute for Computational Biology, Case Western Reserve University, Cleveland, OH, USA

[10]Louis Stokes Cleveland VA Medical Center, Cleveland, OH, USA

[11]Cole Eye Institute, Cleveland Clinic, Cleveland, OH, USA

[12]Department of Pediatrics, The Institute for Translational Genomics and Population Sciences, The Lundquist Institute for Biomedical Innovation at Harbor-UCLA Medical Center, Torrance, CA, USA

[13]Viterbi Family Department of Ophthalmology, Shiley Eye Institute, University of California, San Diego, La Jolla, CA, USA

[14]Department of Ophthalmology and Visual Sciences, Heersink School of Medicine, University of Alabama at Birmingham, Birmingham, AL, USA

[15]Department of Ophthalmology, Columbia University Medical Center, Columbia University, New York, NY, USA

[16]Department of Ophthalmology, University of Nigeria, Ituku, Nigeria

[17]Division of Ophthalmology, Department of Neurosciences, University of the Witwatersrand, Johannesburg, South Africa

[18]Unit of Ophthalmology, Department of Surgery, University of Ghana Medical School, Accra, Ghana

[19]Department of Ophthalmology, University of North Carolina, Chapel Hill, NC, USA

[20]Department of Ophthalmology, University of Ibadan, Ibadan, Nigeria

[21]Sydney Brenner Institute for Molecular Bioscience, Faculty of Health Sciences, University of the Witwatersrand, Johannesburg, South Africa

[22]Department of Epidemiology and Medical Statistics, College of Medicine, University of Ibadan, Ibadan, Nigeria

[23]Singapore Eye Research Institute, Singapore, Singapore

[24]Department of Ophthalmology, Massachusetts Eye and Ear, Harvard Medical School, Boston, MA, USA

[25]Department of Population and Quantitative Health Sciences, Case Western Reserve University, Cleveland, OH, USA

[26]Genome Institute of Singapore, Singapore, Singapore

[27]Department of Medicine, Duke University, Durham, NC, USA

[28]Department of Pharmacology and Toxicology, Center for Health Disparities, Brody School of Medicine. East Carolina University, Greenville, NC, 27834, USA

[29]These authors contributed equally

[30]These authors contributed equally

[31]Lead contact

ACKNOWLEDGMENTS

We greatly appreciate the work of the Clinical Trial Coordinators in the POAAGG study, who made it possible to enroll more than 10,200 individuals of African ancestry in Philadelphia. We acknowledge the Penn Medicine BioBank (PMBB) for providing data and thank the patients of Penn Medicine who consented to participate in this research program. We would also like to thank the Penn Medicine BioBank team and Regeneron Genetics Center for providing genetic variant data for analysis. The PMBB is approved under IRB protocol# 813913 and supported by Perelman School of Medicine at University of Pennsylvania, a gift from the Smilow family, and the National Center for Advancing Translational Sciences of the National Institutes of Health under CTSA award number UL1TR001878. We are grateful to the VA VINCI and GENISIS support and MVP Core Statistical Analysis teams. We would like to thank Dr. Pieter Bonnemaijer for attempting replication of our signals in glaucoma patients from the African descent study (GIGA) dataset. We would also like to thank Dr. Tess Cherlin for support in creating Figure 2, Dr. Theodore Drivas for helping with Figure 3, Sergei Nikonov for helping create Video S1, and Yan Zhu for uploading data to Mendeley Data. Support for title page creation and format was provided by AuthorArranger, a tool developed at the National Cancer Institute. All groups appreciate the critical contribution made by the enrollees. The Primary Open-Angle African American Glaucoma Genetics (POAAGG) study was supported by the National Eye Institute, Bethesda, Maryland (grant #1R01EY023557-01) and the Vision Research Core Grant (P30 EY001583). Funds also come from the F.M. Kirby Foundation, Research to Prevent Blindness, The UPenn Hospital Board of Women Visitors, and The Paul and Evanina Bell Mackall Foundation Trust. Support also came from Regeneron Genetics Center, the Ophthalmology Department at the Perelman School of Medicine, the Genetics Department at the Perelman School of Medicine, and the VA Hospital in Philadelphia, PA. The Genetics of Glaucoma in People of African Descent (GGLAD) study was funded by the National Eye Institute and National Human Genome Research Center (U54HG009826). ADAGES3-Genetics was supported by R01EY023704, and other support included R01EY011008, R01EY019869, R01 EY021818, P30 EY022589, T32 EY026590, and an unrestricted grant from Research to Prevent Blindness (New York, NY). J.I.R. was supported in part by the National Center for Advancing Translational Sciences, CTSI grant UL1TR001881, the National Institute of Diabetes and Digestive and Kidney Disease Diabetes Research Center (DRC) grant DK063491 to the Southern California Diabetes Endocrinology Research, and contract R01EY023704. Infrastructure for the CHARGE Consortium was supported in part by the National Heart, Lung, and Blood Institute (NHLBI) grant R01HL105756. MVP research is based on data from the Million Veteran Program, Office of Research and Development, Veterans Health Administration and was supported by award I01 BX004557. This publication does not represent the views of the Department of Veteran Affairs or the United States Government. This work was also funded by the Cleveland Institute for Computational Biology, NIH Core grants (P30 EY025585 and P30 EY011373) and unrestricted grants from Research to Prevent Blindness to Case Western Reserve University (CWRU) and Cleveland Clinic Lerner College of Medicine of CWRU. J.C.B. and T.G.K. are also supported by NIH R01 EY033829. The sponsor or funding organization had no role in the design or conduct of this research.

DECLARATION OF INTERESTS

J.M.O. is a member of the scientific advisory board of Life Biosciences and a paid consultant of Atheneum Partners, Cerner Enviza (includes Kantar Health), and Calico. A.G.R. holds intellectual property for the use of gene therapy to treat glaucoma. E.M.-E. is a scientific advisor for Avisi and a paid consultant of Aerie Pharmaceuticals, Allergan, Eyenovia, and Thea Pharma. J.L. receives instrument support from Carl Zeiss Meditech, Inc., and Heidelberg Engineering, GmBH; receives research support from Novartis, Inc.; and is a paid consultant at Thea, Inc., Alcon Laboratories, Inc., Johnson & Johnson, Inc., Abbvie, Inc., Carl Zeiss Meditech, Inc., Genetech, Inc., and ONL Therapeutics, Inc.

INCLUSION AND DIVERSITY

We worked to ensure gender balance in the recruitment of human subjects. We worked to ensure ethnic or other types of diversity in the recruitment of human subjects. We worked to ensure that the study questionnaires were prepared in an inclusive way. We worked to ensure diversity in experimental samples through the selection of the cell lines. We worked to ensure diversity in experimental samples through the selection of the genomic datasets. One or more of the authors of this paper self-identifies as an underrepresented ethnic minority in their field of research or within their geographical location. One or more of the authors of this paper self-identifies as a gender minority in their field of research. One or more of the authors of this paper self-identifies as a member of the LGBTQIA+ community. One or more of the authors of this paper self-identifies as living with a disability. One or more of the authors of this paper received support from a program designed to increase minority

representation in their field of research. While citing references scientifically relevant for this work, we also actively worked to promote gender balance in our reference list. We avoided “helicopter science” practices by including the participating local contributors from the region where we conducted the research as authors on the paper.

REFERENCES

1. Weinreb RN, Leung CK, Crowston JG, Medeiros FA, Friedman DS, Wiggs JL, and Martin KR (2016). Primary open-angle glaucoma. Nat. Rev. Dis. Primers 2, 16067. [PubMed: 27654570]
2. Tham YC, Li X, Wong TY, Quigley HA, Aung T, and Cheng CY (2014). Global prevalence of glaucoma and projections of glaucoma burden through 2040: a systematic review and meta-analysis. Ophthalmology 121, 2081–2090. [PubMed: 24974815]
3. Quigley HA, and Broman AT (2006). The number of people with glaucoma worldwide in 2010 and 2020. Br. J. Ophthalmol 90, 262–267. [PubMed: 16488940]
4. Tielsch JM, Katz J, Sommer A, Quigley HA, and Javitt JC (1994). Family history and risk of primary open angle glaucoma. The Baltimore eye survey. Arch. Ophthalmol 112, 69–73. [PubMed: 8285897]
5. Muñoz B, West SK, Rubin GS, Schein OD, Quigley HA, Bressler SB, and Bandeen-Roche K (2000). Causes of blindness and visual impairment in a population of older Americans: the Salisbury Eye Evaluation Study. Arch. Ophthalmol 118, 819–825. [PubMed: 10865321]
6. Janssen SF, Gorgels TG, Ramdas WD, Klaver CC, van Duijn CM, Jansonius NM, and Bergen AA (2013). The vast complexity of primary open angle glaucoma: disease genes, risks, molecular mechanisms and pathobiology. Prog. Retin. Eye Res 37, 31–67. [PubMed: 24055863]
7. Prum BE Jr., Rosenberg LF, Gedde SJ, Mansberger SL, Stein JD, Moroi SE, Herndon LW Jr., Lim MC, and Williams RD (2016). Primary open-angle glaucoma preferred practice pattern® guidelines. Ophthalmology 123, P41–P111. [PubMed: 26581556]
8. Heijl A, Bengtsson B, Hyman L, and Leske MC; Early Manifest Glaucoma Trial Group (2009). Natural history of open-angle glaucoma. Ophthalmology 116, 2271–2276. [PubMed: 19854514]
9. Anderson DR, Drance SM, and Schulzer M; Collaborative Normal-Tension Glaucoma Study Group (2001). Natural history of normal-tension glaucoma. Ophthalmology 108, 247–253. [PubMed: 11158794]
10. Heijl A, Leske MC, Bengtsson B, Hyman L, Bengtsson B, and Hussein M; Early Manifest Glaucoma Trial Group (2002). Reduction of intraocular pressure and glaucoma progression: results from the Early Manifest Glaucoma Trial. Arch. Ophthalmol 120, 1268–1279. [PubMed: 12365904]
11. Gordon MO, Beiser JA, Brandt JD, Heuer DK, Higginbotham EJ, Johnson CA, Keltner JL, Miller JP, Parrish RK 2nd, Wilson MR, et al. (2002). The Ocular Hypertension Treatment Study: baseline factors that predict the onset of primary open-angle glaucoma. Arch. Ophthalmol 120. 714–20; discussion 829. [PubMed: 12049575]
12. Leske MC, Wu SY, Hennis A, Honkanen R, and Nemesure B; Bess Study Group (2008). Risk factors for incident open-angle glaucoma: the Barbados Eye Studies. Ophthalmology 115, 85–93. [PubMed: 17629563]
13. O’Brien JM, Salowe RJ, Fertig R, Salinas J, Pistilli M, Sankar PS, Miller-Ellis E, Lehman A, Murphy WHA, Homsher M, et al. (2018). Family history in the primary open-angle African American glaucoma genetics study cohort. Am. J. Ophthalmol 192, 239–247. [PubMed: 29555482]
14. Teikari JM (1987). Genetic factors in open-angle (simple and capsular) glaucoma. A population-based twin study. Acta Ophthalmol. (Copenh) 65, 715–720. [PubMed: 3434238]
15. Gottfredsdottir MS, Sverrisson T, Musch DC, and Stefansson E (1999). Chronic open-angle glaucoma and associated ophthalmic findings in monozygotic twins and their spouses in Iceland. J. Glaucoma 8, 134–139. [PubMed: 10209731]
16. Liu Y, and Allingham RR (2017). Major review: molecular genetics of primary open-angle glaucoma. Exp. Eye Res 160, 62–84. [PubMed: 28499933]

17. Zhou W, Kanai M, Wu KH, Rasheed H, Tsuo K, Hirbo JB, Wang Y, Bhattacharya A, Zhao H, Namba S, et al. (2022). Global biobank Meta-analysis Initiative: powering genetic discovery across human disease. Cell Genomics 2, 100192. [PubMed: 36777996]

18. Burdon KP, Macgregor S, Hewitt AW, Sharma S, Chidlow G, Mills RA, Danoy P, Casson R, Viswanathan AC, Liu JZ, et al. (2011). Genome-wide association study identifies susceptibility loci for open angle glaucoma at TMCO1 and CDKN2B-AS1. Nat. Genet 43, 574–578. [PubMed: 21532571]

19. Gibson J, Griffiths H, De Salvo G, Cole M, Jacob A, Macleod A, Yang Y, Menon G, Cree A, Ennis S, et al. (2012). Genome-wide association study of primary open angle glaucoma risk and quantitative traits. Mol. Vis 18, 1083–1092. [PubMed: 22605921]

20. Thorleifsson G, Magnusson KP, Sulem P, Walters GB, Gudbjartsson DF, Stefansson H, Jonsson T, Jonasdottir A, Jonasdottir A, Stefansdottir G, et al. (2007). Common sequence variants in the LOXL1 gene confer susceptibility to exfoliation glaucoma. Science 317, 1397–1400. [PubMed: 17690259]

21. Thorleifsson G, Walters GB, Hewitt AW, Masson G, Helgason A, DeWan A, Sigurdsson A, Jonasdottir A, Gudjonsson SA, Magnusson KP, et al. (2010). Common variants near CAV1 and CAV2 are associated with primary open-angle glaucoma. Nat. Genet 42, 906–909. [PubMed: 20835238]

22. Wiggs JL, Yaspan BL, Hauser MA, Kang JH, Allingham RR, Olson LM, Abdrabou W, Fan BJ, Wang DY, Brodeur W, et al. (2012). Common variants at 9p21 and 8q22 are associated with increased susceptibility to optic nerve degeneration in glaucoma. PLoS Genet. 8, e1002654. [PubMed: 22570617]

23. Nakano M, Ikeda Y, Taniguchi T, Yagi T, Fuwa M, Omi N, Tokuda Y, Tanaka M, Yoshii K, Kageyama M, et al. (2009). Three susceptible loci associated with primary open-angle glaucoma identified by genome-wide association study in a Japanese population. Proc. Natl. Acad. Sci. USA 106, 12838–12842. [PubMed: 19625618]

24. Nakano M, Ikeda Y, Tokuda Y, Fuwa M, Omi N, Ueno M, Imai K, Adachi H, Kageyama M, Mori K, et al. (2012). Common variants in CDKN2B-AS1 associated with optic-nerve vulnerability of glaucoma identified by genome-wide association studies in Japanese. PLoS One 7, e33389. [PubMed: 22428042]

25. Osman W, Low SK, Takahashi A, Kubo M, and Nakamura Y (2012). A genome-wide association study in the Japanese population confirms 9p21 and 14q23 as susceptibility loci for primary open angle glaucoma. Hum. Mol. Genet 21, 2836–2842. [PubMed: 22419738]

26. Takamoto M, Kaburaki T, Mabuchi A, Araie M, Amano S, Aihara M, Tomidokoro A, Iwase A, Mabuchi F, Kashiwagi K, et al. (2012). Common variants on chromosome 9p21 are associated with normal tension glaucoma. PLoS One 7, e40107. [PubMed: 22792221]

27. Inoko AH, Ota M, Mizuki N, and Bahram S (2010). Genome-wide association study of normal tension glaucoma: common variants in SRBD1 and ELOVL5 contribute to disease susceptibility. Ophthalmology 117, 1331–1338.e5. [PubMed: 20363506]

28. Bailey JN, Loomis SJ, Kang JH, Allingham RR, Gharahkhani P, Khor CC, Burdon KP, Aschard H, Chasman DI, Igo RP Jr., et al. (2016). Genome-wide association analysis identifies TXNRD2, ATXN2 and FOXC1 as susceptibility loci for primary open-angle glaucoma. Nat. Genet 48, 189–194. [PubMed: 26752265]

29. Gharahkhani P, Jorgenson E, Hysi P, Khawaja AP, Pendergrass S, Han X, Ong JS, Hewitt AW, Segrè AV, Rouhana JM, et al. (2021). Genome-wide meta-analysis identifies 127 open-angle glaucoma loci with consistent effect across ancestries. Nat. Commun 12, 1258. [PubMed: 33627673]

30. Hoffmann TJ, Tang H, Thornton TA, Caan B, Haan M, Millen AE, Thomas F, and Risch N (2014). Genome-wide association and admixture analysis of glaucoma in the Women's Health Initiative. Hum. Mol. Genet 23, 6634–6643. [PubMed: 25027321]

31. Bonnemaijer PWM, Iglesias AI, Nadkarni GN, Sanyiwa AJ, Hassan HG, Cook C, GIGA Study Group, Simcoe M, Taylor KD, Schurmann C, et al. (2018). Genome-wide association study of primary openangle glaucoma in continental and admixed African populations. Hum. Genet 137, 847–862. [PubMed: 30317457]

32. Liu Y, Hauser MA, Akafo SK, Qin X, Miura S, Gibson JR, Wheeler J, Gaasterland DE, Challa P, Herndon LW, et al. (2013). Investigation of known genetic risk factors for primary open angle glaucoma in two populations of African ancestry. Invest. Ophthalmol. Vis. Sci 54, 6248–6254. [PubMed: 23963167]
33. Choquet H, Paylakhi S, Kneeland SC, Thai KK, Hoffmann TJ, Yin J, Kvale MN, Banda Y, Tolman NG, Williams PA, et al. (2018). A multiethnic genome-wide association study of primary open-angle glaucoma identifies novel risk loci. Nat. Commun 9, 2278. [PubMed: 29891935]
34. Gharahkhani P, Burdon KP, Cooke Bailey JN, Hewitt AW, Law MH, Pasquale LR, Kang JH, Haines JL, Souzeau E, Zhou T, et al. (2018). Analysis combining correlated glaucoma traits identifies five new risk loci for open-angle glaucoma. Sci. Rep 8, 3124. [PubMed: 29449654]
35. Zangwill LM, Ayyagari R, Liebmann JM, Girkin CA, Feldman R, Dubiner H, Dirkes KA, Holmann M, Williams-Steppe E, Hammel N, et al. (2019). The African Descent and Glaucoma Evaluation Study (ADAGES) III: Contribution of genotype to glaucoma phenotype in African Americans: study design and baseline data. Ophthalmology 126, 156–170. [PubMed: 29361356]
36. Taylor KD, Guo X, Zangwill LM, Liebmann JM, Girkin CA, Feldman RM, Dubiner H, Hai Y, Samuels BC, Panarelli JF, et al. (2019). Genetic architecture of primary open-angle glaucoma in individuals of African descent: the African descent and glaucoma evaluation Study III. Ophthalmology 126, 38–48. [PubMed: 30352225]
37. Genetics of Glaucoma in People of African Descent (GGLAD) Consortium, Hauser MA, Allingham RR, Aung T, Van Der Heide CJ, Taylor KD, Rotter JI, Wang SJ, Bonnemaijer PWM, Williams SE, et al. (2019). Association of genetic variants with primary open-angle glaucoma among individuals with African Ancestry. JAMA 322, 1682–1691. [PubMed: 31688885]
38. Charlson ES, Sankar PS, Miller-Ellis E, Regina M, Fertig R, Salinas J, Pistilli M, Salowe RJ, Rhodes AL, Merritt WT 3rd., et al. (2015). The primary open-angle African American glaucoma genetics study: baseline demographics. Ophthalmology 122, 711–720. [PubMed: 25576993]
39. Das S, Forer L, Schönherr S, Sidore C, Locke AE, Kwong A, Vrieze SI, Chew EY, Levy S, McGue M, et al. (2016). Next-generation genotype imputation service and methods. Nat. Genet 48, 1284–1287. [PubMed: 27571263]
40. All of Us Research Program Investigators, Denny JC, Rutter JL, Goldstein DB, Philippakis A, Smoller JW, Jenkins G, and Dishman E (2019). The “all of us” research program. N. Engl. J. Med 381, 668–676. [PubMed: 31412182]
41. Lau-Min KS, Asher SB, Chen J, Domchek SM, Feldman M, Joffe S, Landgraf J, Speare V, Varughese LA, Tuteja S, et al. (2021). Real-world integration of genomic data into the electronic health record: the PennChart Genomics Initiative. Genet. Med 23, 603–605. [PubMed: 33299147]
42. Gaziano JM, Concato J, Brophy M, Fiore L, Pyarajan S, Breeling J, Whitbourne S, Deen J, Shannon C, Humphries D, et al. (2016). Million Veteran Program: a mega-biobank to study genetic influences on health and disease. J. Clin. Epidemiol 70, 214–223. [PubMed: 26441289]
43. Welter D, MacArthur J, Morales J, Burdett T, Hall P, Junkins H, Klemm A, Flicek P, Manolio T, Hindorff L, et al. (2014). The NHGRI GWAS Catalog, a curated resource of SNP-trait associations. Nucleic Acids Res. 42, D1001–D1006. [PubMed: 24316577]
44. Yang J, Lee SH, Goddard ME, and Visscher PM (2011). GCTA: a tool for genome-wide complex trait analysis. Am. J. Hum. Genet 88, 76–82. [PubMed: 21167468]
45. Yang J, Ferreira T, Morris AP, Medland SE, Genetic Investigation of ANthropometric Traits (GIANT) Consortium; DIAbetes Genetics Replication And Meta-analysis (DIAGRAM) Consortium, Madden, P.A.F., Health AC, Martin NG, Montgomery GW, et al. (2012). Conditional and joint multiple-SNP analysis of GWAS summary statistics identifies additional variants influencing complex traits. Nat. Genet. 44, 369–375. [PubMed: 22426310]
46. Springelkamp H, Iglesias AI, Cuellar-Partida G, Amin N, Burdon KP, van Leeuwen EM, Gharahkhani P, Mishra A, van der Lee SJ, Hewitt AW, et al. (2015). ARHGEF12 influences the risk of glaucoma by increasing intraocular pressure. Hum. Mol. Genet 24, 2689–2699. [PubMed: 25637523]
47. Gharahkhani P, Burdon KP, Fogarty R, Sharma S, Hewitt AW, Martin S, Law MH, Cremin K, Bailey JNC, Loomis SJ, et al. (2014). Common variants near ABCA1, AFAP1 and GMDS confer risk of primary open-angle glaucoma. Nat. Genet 46, 1120–1125. [PubMed: 25173105]

48. Morales J, Al-Sharif L, Khalil DS, Shinwari JMA, Bavi P, Al-Mahrouqi RA, Al-Rajhi A, Alkuraya FS, Meyer BF, and Al Tassan N (2009). Homozygous mutations in ADAMTS10 and ADAMTS17 cause lenticular myopia, ectopia lentis, glaucoma, spherophakia, and short stature. Am. J. Hum. Genet 85, 558–568. [PubMed: 19836009]
49. Marzin P, Cormier-Daire V, and Tsilou E (1993). Weill-Marchesani syndrome. In GeneReviews, Adam MP, Mirzaa GM, Pagon RA, Wallace SE, Bean LJH, Gripp KW, and Amemiya A, eds. (University of Washington).
50. Yamagata M, and Sanes JR (2018). Expression and roles of the immunoglobulin superfamily recognition molecule Sidekick1 in mouse retina. Front. Mol. Neurosci 11, 485. [PubMed: 30687002]
51. Foley CN, Staley JR, Breen PG, Sun BB, Kirk PDW, Burgess S, and Howson JMM (2021). A fast and efficient colocalization algorithm for identifying shared genetic risk factors across multiple traits. Nat. Commun 12, 764. [PubMed: 33536417]
52. Brown BC, Asian Genetic Epidemiology Network Type 2 Diabetes Consortium, Ye CJ, Price AL, and Zaitlen N (2016). Transethnic Genetic-Correlation Estimates from Summary Statistics. Am. J. Hum. Genet 99, 76–88. [PubMed: 27321947]
53. Lee SH, Wray NR, Goddard ME, and Visscher PM (2011). Estimating missing heritability for disease from genome-wide association studies. Am. J. Hum. Genet 88, 294–305. [PubMed: 21376301]
54. Li D, Hsu S, Purushotham D, Sears RL, and Wang T (2019). WashU epigenome Browser update 2019. Nucleic Acids Res. 47, W158–W165. [PubMed: 31165883]
55. Boix CA, James BT, Park YP, Meuleman W, and Kellis M (2021). Regulatory genomic circuitry of human disease loci by integrative epigenomics. Nature 590, 300–307. [PubMed: 33536621]
56. Weissbrod O, Hormozdiari F, Benner C, Cui R, Ulirsch J, Gazal S, Schoech AP, van de Geijn B, Reshef Y, Márquez-Luna C, et al. (2020). Functionally informed fine-mapping and polygenic localization of complex trait heritability. Nat. Genet 52, 1355–1363. [PubMed: 33199916]
57. Pressman CL, Chen H, and Johnson RL (2000). LMX1B, a LIM homeodomain class transcription factor, is necessary for normal development of multiple tissues in the anterior segment of the murine eye. Genesis 26, 15–25. [PubMed: 10660670]
58. Ham JH, Shin SJ, Joo KR, Park SM, Sung HY, Kim JS, Choi JS, Choi YJ, Song HC, and Choi EJ (2009). A synonymous genetic alteration of LMX1B in a family with nail-patella syndrome. Korean J. Intern. Med 24, 274–278. [PubMed: 19721866]
59. Haro E, Petit F, Pira CU, Spady CD, Lucas-Toca S, Yorozuya LI, Gray AL, Escande F, Jourdain AS, Nguyen A, et al. (2021). Identification of limb-specific Lmx1b auto-regulatory modules with nail-patella syndrome pathogenicity. Nat. Commun 12, 5533. [PubMed: 34545091]
60. Mimiwati Z, Mackey DA, Craig JE, Mackinnon JR, Rait JL, Liebelt JE, Ayala-Lugo R, Vollrath D, and Richards JE (2006). Nail-patella syndrome and its association with glaucoma: a review of eight families. Br. J. Ophthalmol 90, 1505–1509. [PubMed: 16825280]
61. Yan X, Lin J, Wang Y, Xuan J, Yu P, Guo T, and Jin F (2019). A novel small deletion of LMX1B in a large Chinese family with nail-patella syndrome. BMC Med. Genet 20, 71. [PubMed: 31053111]
62. Vollrath D, Jaramillo-Babb VL, Clough MV, McIntosh I, Scott KM, Lichter PR, and Richards JE (1998). Loss-of-function mutations in the LIM-homeodomain gene, LMX1B, in nail-patella syndrome. Hum. Mol. Genet 7, 1091–1098. [PubMed: 9618165]
63. Lichter PR, Richards JE, Downs CA, Stringham HM, Boehnke M, and Farley FA (1997). Cosegregation of open-angle glaucoma and the nail-patella syndrome. Am. J. Ophthalmol 124, 506–515. [PubMed: 9323941]
64. Idaghdour Y, Czika W, Shianna KV, Lee SH, Visscher PM, Martin HC, Miclaus K, Jadallah SJ, Goldstein DB, Wolfinger RD, et al. (2010). Geographical genomics of human leukocyte gene expression variation in southern Morocco. Nat. Genet 42, 62–67. [PubMed: 19966804]
65. Watanabe K, Taskesen E, van Bochoven A, and Posthuma D (2017). Functional mapping and annotation of genetic associations with FUMA. Nat. Commun 8, 1826. [PubMed: 29184056]
66. de Leeuw CA, Mooij JM, Heskes T, and Posthuma D (2015). MAGMA: generalized gene-set analysis of GWAS data. PLoS Comput. Biol 11, e1004219. [PubMed: 25885710]

67. Liberzon A, Birger C, Thorvaldsdóttir H, Ghandi M, Mesirov JP, and Tamayo P (2015). The Molecular Signatures Database (MSigDB) hallmark gene set collection. Cell. Syst 1, 417–425. [PubMed: 26771021]
68. Agarwal R, Gupta SK, Agarwal P, Saxena R, and Agrawal SS (2009). Current concepts in the pathophysiology of glaucoma. Indian J. Ophthalmol 57, 257–266. [PubMed: 19574692]
69. Chavali VRM, Haider N, Rathi S, Alapati T, He J, Gill K, Nikonov S, Nikonov R, Duong TT, McDougald DS, et al. (2020). Dual SMAD inhibition and Wnt inhibition enhances the differentiation of induced pluripotent stem cells into retinal ganglion cells. Sci. Rep 10, 11828. [PubMed: 32678240]
70. Wolf J, Boneva S, Schlecht A, Lapp T, Auw-Haedrich C, Lagrèze W, Agostini H, Reinhard T, Schlunck G, and Lange C (2022). The Human Eye Transcriptome Atlas: a searchable comparative transcriptome database for healthy and diseased human eye tissue. Genomics 114, 110286. [PubMed: 35124170]
71. Wolf J, Lapp T, Reinhard T, Agostini H, Schlunck G, and Lange C (2022). Web-based gene expression analysis-paving the way to decode healthy and diseased ocular tissue. Ophthalmologie 119, 929–936. [PubMed: 35194679]
72. GTEx Consortium (2013). The Genotype-Tissue Expression (GTEx) project. Nat. Genet 45, 580–585. [PubMed: 23715323]
73. ENCODE Project Consortium (2012). An integrated encyclopedia of DNA elements in the human genome. Nature 489, 57–74. [PubMed: 22955616]
74. Sirugo G, Williams SM, and Tishkoff SA (2019). The missing diversity in human genetic studies. Cell 177, 26–31. [PubMed: 30901543]
75. Rao VP, and Epstein DL (2007). Rho GTPase/Rho kinase inhibition as a novel target for the treatment of glaucoma. BioDrugs 21, 167–177. [PubMed: 17516712]
76. Wang J, Liu X, and Zhong Y (2013). Rho/Rho-associated kinase pathway in glaucoma (Review). Int. J. Oncol 43, 1357–1367. [PubMed: 24042317]
77. Tanna AP, and Johnson M (2018). Rho kinase inhibitors as a novel treatment for glaucoma and ocular hypertension. Ophthalmology 125, 1741–1756. [PubMed: 30007591]
78. Pattabiraman PP, Maddala R, and Rao PV (2014). Regulation of plasticity and fibrogenic activity of trabecular meshwork cells by Rho GTPase signaling. J. Cell. Physiol 229, 927–942. [PubMed: 24318513]
79. Fukata Y, Amano M, and Kaibuchi K (2001). Rho-Rho-kinase pathway in smooth muscle contraction and cytoskeletal reorganization of non-muscle cells. Trends Pharmacol. Sci 22, 32–39. [PubMed: 11165670]
80. Honjo M, Tanihara H, Inatani M, Kido N, Sawamura T, Yue BY, Narumiya S, and Honda Y (2001). Effects of rho-associated protein kinase inhibitor Y-27632 on intraocular pressure and outflow facility. Invest. Ophthalmol. Vis. Sci 42, 137–144. [PubMed: 11133858]
81. Kumar J, and Epstein DL (2011). Rho GTPase-mediated cytoskeletal organization in Schlemm's canal cells play a critical role in the regulation of aqueous humor outflow facility. J. Cell. Biochem 112, 600–606. [PubMed: 21268081]
82. Lessey-Morillon EC, Osborne LD, Monaghan-Benson E, Guilluy C, O'Brien ET, Superfine R, and Burridge K (2014). The RhoA guanine nucleotide exchange factor, LARG, mediates ICAM-1-dependent mechanotransduction in endothelial cells to stimulate transendothelial migration. J. Immunol 192, 3390–3398. [PubMed: 24585879]
83. Okuhira K, Fitzgerald ML, Tamehiro N, Ohoka N, Suzuki K, Sawada J, Naito M, and Nishimaki-Mogami T (2010). Binding of PDZ-RhoGEF to ATP-binding cassette transporter A1 (ABCA1) induces cholesterol efflux through RhoA activation and prevention of transporter degradation. J. Biol. Chem 285, 16369–16377. [PubMed: 20348106]
84. Trivli A, Zervou MI, Goulielmos GN, Spandidos DA, and Detorakis ET (2020). Primary open angle glaucoma genetics: the common variants and their clinical associations (Review). Mol. Med. Rep 22, 1103–1110. [PubMed: 32626970]
85. Iglesias AI, Springelkamp H, Ramdas WD, Klaver CCW, Willemsen R, and van Duijn CM (2015). Genes, pathways, and animal models in primary open-angle glaucoma. Eye (Lond.) 29, 1285–1298. [PubMed: 26315706]

86. Fuchshofer R, and Tamm ER (2012). The role of TGF-b in the pathogenesis of primary open-angle glaucoma. Cell Tissue Res 347, 279–290. [PubMed: 22101332]

87. Wordinger RJ, Sharma T, and Clark AF (2014). The role of TGF-b2 and bone morphogenetic proteins in the trabecular meshwork and glaucoma. J. Ocul. Pharmacol. Ther 30, 154–162. [PubMed: 24517218]

88. Fleenor DL, Shepard AR, Hellberg PE, Jacobson N, Pang IH, and Clark AF (2006). TGFbeta2-induced changes in human trabecular meshwork: implications for intraocular pressure. Invest. Ophthalmol. Vis. Sci 47, 226–234. [PubMed: 16384967]

89. Cousins SW, McCabe MM, Danielpour D, and Streilein JW (1991). Identification of transforming growth factor-beta as an immunosuppressive factor in aqueous humor. Invest. Ophthalmol. Vis. Sci 32, 2201–2211. [PubMed: 2071334]

90. Jampel HD, Roche N, Stark WJ, and Roberts AB (1990). Transforming growth factor-beta in human aqueous humor. Curr. Eye Res 9, 963–969. [PubMed: 2276273]

91. Min SH, Lee TI, Chung YS, and Kim HK (2006). Transforming growth factor-beta levels in human aqueous humor of glaucomatous, diabetic and uveitic eyes. Korean J. Ophthalmol 20, 162–165. [PubMed: 17004630]

92. Pena JD, Taylor AW, Ricard CS, Vidal I, and Hernandez MR (1999). Transforming growth factor beta isoforms in human optic nerve heads. Br. J. Ophthalmol 83, 209–218. [PubMed: 10396201]

93. Waksmunski AR, Kinzy TG, Cruz LA, Nealon CL, Halladay CW, Simpson P, Canania RL, Anthony SA, Roncone DP, Sawicki Rogers L, et al. (2022). Glaucoma genetic risk scores in the Million Veteran Program. Ophthalmology 129, 1263–1274. [PubMed: 35718050]

94. Xiao R, and Boehnke M (2009). Quantifying and correcting for the winner's curse in genetic association studies. Genet. Epidemiol 33, 453–462. [PubMed: 19140131]

95. Major; Depressive; Disorder Working Group of the Psychiatric; GWAS Consortium, Ripke S, Wray NR, Lewis CM, Hamilton SP, Weissman MM, Breen G, Byrne EM, Blackwood DH, Boomsma DI, et al. (2013). A mega-analysis of genome-wide association studies for major depressive disorder. Mol. Psychiatry 18, 497–511. [PubMed: 22472876]

96. Gorski M, Günther F, Winkler TW, Weber BHF, and Heid IM (2019). On the differences between mega- and meta-imputation and analysis exemplified on the genetics of age-related macular degeneration. Genet. Epidemiol 43, 559–576. [PubMed: 31016765]

97. Doucette LP, Rasnitsyn A, Seifi M, and Walter MA (2015). The interactions of genes, age, and environment in glaucoma pathogenesis. Surv. Ophthalmol 60, 310–326. [PubMed: 25907525]

98. Cooke Bailey JN, Funk KL, Cruz LA, Waksmunski AR, Kinzy TG, Wiggs JL, and Hauser MA (2022). Diversity in polygenic risk of primary open-angle glaucoma. Genes (Basel) 14, 111. [PubMed: 36672852]

99. Verma SS, de Andrade M, Tromp G, Kuivaniemi H, Pugh E, Namjou-Khales B, Mukherjee S, Jarvik GP, Kottyan LC, Burt A, et al. (2014). Imputation and quality control steps for combining multiple genome-wide datasets. Front. Genet 5, 370. [PubMed: 25566314]

100. Stanaway IB, Hall TO, Rosenthal EA, Palmer M, Naranbhai V, Knevel R, Namjou-Khales B, Carroll RJ, Kiryluk K, Gordon AS, et al. (2019). The eMERGE genotype set of 83,717 subjects imputed to ^40 million variants genome wide and association with the herpes zoster medical record phenotype. Genet. Epidemiol 43, 63–81. [PubMed: 30298529]

101. Galinsky KJ, Loh PR, Mallick S, Patterson NJ, and Price AL (2016). Population structure of UK Biobank and ancient eurasians reveals adaptation at genes influencing blood pressure. Am. J. Hum. Genet 99, 1130–1139. [PubMed: 27773431]

102. Galinsky KJ, Bhatia G, Loh PR, Georgiev S, Mukherjee S, Patterson NJ, and Price AL (2016). Fast principal-component analysis reveals convergent evolution of ADH1B in Europe and East Asia. Am. J. Hum. Genet 98, 456–472. [PubMed: 26924531]

103. Mbatchou J, Barnard L, Backman J, Marcketta A, Kosmicki JA, Ziyatdinov A, Benner C, O'Dushlaine C, Barber M, Boutkov B, et al. (2021). Computationally efficient whole-genome regression for quantitative and binary traits. Nat. Genet 53, 1097–1103. [PubMed: 34017140]

104. Boughton AP, Welch RP, Flickinger M, VandeHaar P, Taliun D, Abecasis GR, and Boehnke M (2021). LocusZoom.js: interactive and embeddable visualization of genetic association study results. Bioinformatics 37, 3017–3018. [PubMed: 33734315]

105. Zheng J, Erzurumluoglu AM, Elsworth BL, Kemp JP, Howe L, Haycock PC, Hemani G, Tansey K, Laurin C, et al. ; Early Genetics and Lifecourse Epidemiology (EAGLE) Eczema Consortium (2017). LD Hub: a centralized database and web interface to perform LD score regression that maximizes the potential of summary level GWAS data for SNP heritability and genetic correlation analysis. Bioinformatics 33, 272–279. [PubMed: 27663502]
106. Bulik-Sullivan BK, Loh PR, Finucane HK, Ripke S, Yang J, Schizophrenia Working Group of the Psychiatric; Genomics Consortium, Patterson N, Daly MJ, Price AL, and Neale BM (2015). LD Score regression distinguishes confounding from polygenicity in genomewide association studies. Nat. Genet 47, 291–295. [PubMed: 25642630]
107. Chang CC, Chow CC, Tellier LC, Vattikuti S, Purcell SM, and Lee JJ (2015). Second-generation PLINK: rising to the challenge of larger and richer datasets. GigaScience 4,7. [PubMed: 25722852]
108. Verkuil L, Danford I, Pistilli M, Collins DW, Gudiseva HV, Trachtman BT, He J, Rathi S, Haider N, Ying GS, et al. (2019). SNP located in an AluJb repeat downstream of TMCO1, rs4657473, is protective for POAG in African Americans. Br. J. Ophthalmol 103, 1530–1536. [PubMed: 30862618]
109. Gudiseva HV, Vrathasha V, He J, Bungatavula D, O'Brien JM, and Chavali VRM (2021). Single cell sequencing of induced pluripotent stem cell derived retinal ganglion cells (iPSC-RGC) reveals distinct molecular signatures and RGC subtypes. Genes (Basel) 12, 2015. [PubMed: 34946963]
110. Vrathasha V, Nikonov S, Bell BA, He J, Bungatavula Y, Uyhazi KE, and Murthy Chavali VR (2022). Transplanted human induced pluripotent stem cells-derived retinal ganglion cells embed within mouse retinas and are electrophysiologically functional. iScience 25, 105308. [PubMed: 36388952]
111. Girkin CA, Nievergelt CM, Kuo JZ, Maihofer AX, Huisingh C, Liebmann JM, Ayyagari R, Weinreb RN, Ritch R, Zangwill LM, et al. (2015). Biogeographic ancestry in the African Descent and Glaucoma Evaluation Study (ADAGES): association with corneal and optic nerve structure. Invest. Ophthalmol. Vis. Sci 56, 2043–2049. [PubMed: 25744975]
112. Plagnol V, Smyth DJ, Todd JA, and Clayton DG (2009). Statistical independence of the colocalized association signals for type 1 diabetes and RPS26 gene expression on chromosome 12q13. Biostatistics 10, 327–334. [PubMed: 19039033]
113. Wallace C (2013). Statistical testing of shared genetic control for potentially related traits. Genet. Epidemiol 37, 802–813. [PubMed: 24227294]
114. Drivas TG, Lucas A, and Ritchie MD (2021). eQTpLot: a user-friendly R package for the visualization of colocalization between eQTL and GWAS signals. BioData Min. 14, 32. [PubMed: 34273980]
115. Kang EY, Park Y, Li X, Segre AV, Han B, and Eskin E (2016). ForestPMPlot: a flexible tool for visualizing heterogeneity between studies in meta-analysis. G3 (Bethesda) 6, 1793–1798. [PubMed: 27194809]
116. Faro VL, Bhattacharya A, Zhou W, Zhou D, Wang Y, Läll K, Kanai M, Lopera-Maya E, Straub P, Pawar P, et al. (2022). Genome-wide association meta-analysis identifies novel ancestry-specific primary open-angle glaucoma loci and shared biology with vascular mechanisms and cell proliferation. Preprint at medRxiv.
117. 1000 Genomes Project Consortium, Auton A, Brooks LD, Durbin RM, Garrison EP, Kang HM, Korbel JO, Marchini JL, McCarthy S, McVean GA, et al. (2015). A global reference for human genetic variation. Nature 526, 68–74. [PubMed: 26432245]
118. Tezel G, Yang X, Luo C, Kain AD, Powell DW, Kuehn MH, and Kaplan HJ (2010). Oxidative stress and the regulation of complement activation in human glaucoma. Invest. Ophthalmol. Vis. Sci 51, 5071–5082. [PubMed: 20484586]
119. Benoist d'Azy C, Pereira B, Chiambaretta F, and Dutheil F (2016). Oxidative and anti-oxidative stress markers in chronic glaucoma: a systematic review and meta-analysis. PLoS One 11, e0166915. [PubMed: 27907028]
120. Wang M, and Zheng Y (2019). Oxidative stress and antioxidants in the trabecular meshwork. PeerJ 7, e8121. [PubMed: 31788363]

121. Ge T, Chen CY, Ni Y, Feng YA, and Smoller JW (2019). Polygenic prediction via Bayesian regression and continuous shrinkage priors. Nat. Commun 10, 1776. [PubMed: 30992449]

122. Verma A, Damrauer SM, Naseer N, Weaver J, Kripke CM, Guare L, Sirugo G, Kember RL, Drivas TG, Dudek SM, et al. (2022). The Penn Medicine biobank: towards a genomics-enabled learning healthcare system to accelerate precision Medicine in a diverse population. J. Pers. Med 12, 1974. [PubMed: 36556195]

Highlights

- A comprehensive GWAS on African ancestry individuals with glaucoma was conducted
- 46 risk loci significantly associated with glaucoma were detected
- Variants in *ROCK1P1, ARHGEF12*, and *DBF4P2* demonstrated likely causal pathophysiology
- Polygenic risk scores derived from African ancestry individuals show enhanced strength

	STUDY DESIGN						STUDY PARTICIPANT CHARACTERISTICS			
	Data	Study Location	#Cases	N	Cases/Controls	Variants Evaluated	Ancestry	% of Cohort that identify as African ancestry	Age *mean*	% Female
Discovery	POAAGG	Philadelphia	2,710	6,324		13,944,299	Self-identified as Black *African American, African descent, or African Caribbean*		65	
	ADAGES	California, New York, Alabama, Texas & Georgia	1,823	1,999		13,944,299	Self-identified as African ancestry		67.2	
	GGLAD - 1 AFR	United States	705	1,312		13,944,299	Self-identified as African ancestry		61.2	
	GGLAD - 1 Ghana	Ghana	640	1,330		13,944,299	Continental African		59.6	
	GGLAD - 1 Nigeria	Nigeria	125	310		13,944,299	Continental African		63.2	
Replication	GGLAD- 2	United States, Ghana, Nigeria & South Africa	851	1,492		353	Continental African or self-identified as African ancestry			
	All of Us	United States	772	22,914		353	Genetically determined African ancestry		51.6	
	Penn Medicine BioBank	Philadelphia	356	9,512		353	Self identified as Black		51.6	
	Million Veterans Program	United States	3,921	9,586		353	Self-identified as Black and confirmed via genetic ancestry		68.9	
Comparative Analyses	GBMI - EUR	Multiple	16,355	1,172,899		5,257,495	Genetically determined European *Non-Finnish European*			
	GBMI - EAS	Japan & Taiwan	9,715	269,960		5,257,495	Genetically determined East Asian ancestry			
	GBMI - All	Multiple	26,848	1,487,447		5,257,495	Genetically determined ancestries *EAS, AFR, AMR, EUR, SAS*			

Figure 1. Study designs and subject characteristics

POAAGG, Primary Open-Angle African American Glaucoma Genetics; GGLAD, Genetics of Glaucoma in People of African Descent; ADAGES, African Descent and Glaucoma Evaluation Study; AOU, All of Us; GBMI, Global BioBank Meta-Analysis Initiative; EAS, East Asian Ancestry; AFR, African Ancestry; AMR, Admixed American Ancestry; EUR, European Ancestry; SAS, South Asian Ancestry.

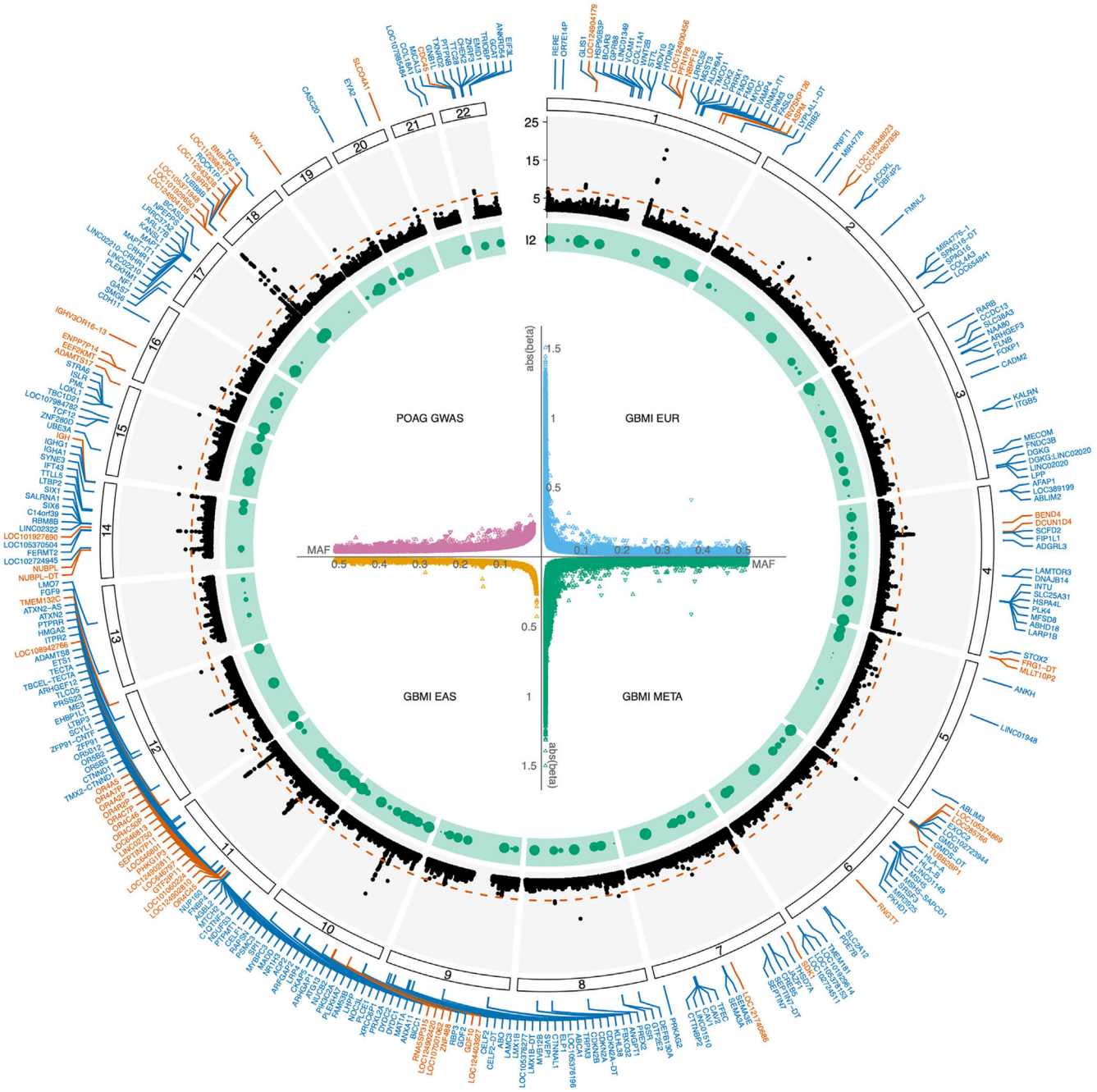

Figure 2. Discovery of known and previously undescribed loci from the discovery mega-analysis of African ancestry individuals

For a Figure360 author presentation of this figure, see https://doi.org/10.1016/j.cell.2023.12.006.

The circular plot depicts genes previously associated with POAG (blue) and previously undescribed genes revealed by the discovery mega-analysis (orange). The inner section (black) shows the mega-analysis Manhattan plot in a circular fashion. The green section demonstrates heterogeneity I2 values from sex-stratified meta-analyses. The inner scatter plots display the relationship between the absolute beta and minor allele frequency (MAF)

among the mega-analysis data, including African ancestry individuals only and GBMI results for European individuals, East Asian individuals, and cross-ancestry meta-analyses. See also Tables S1–S4 and S7 and Figures S1, S2, and S4.

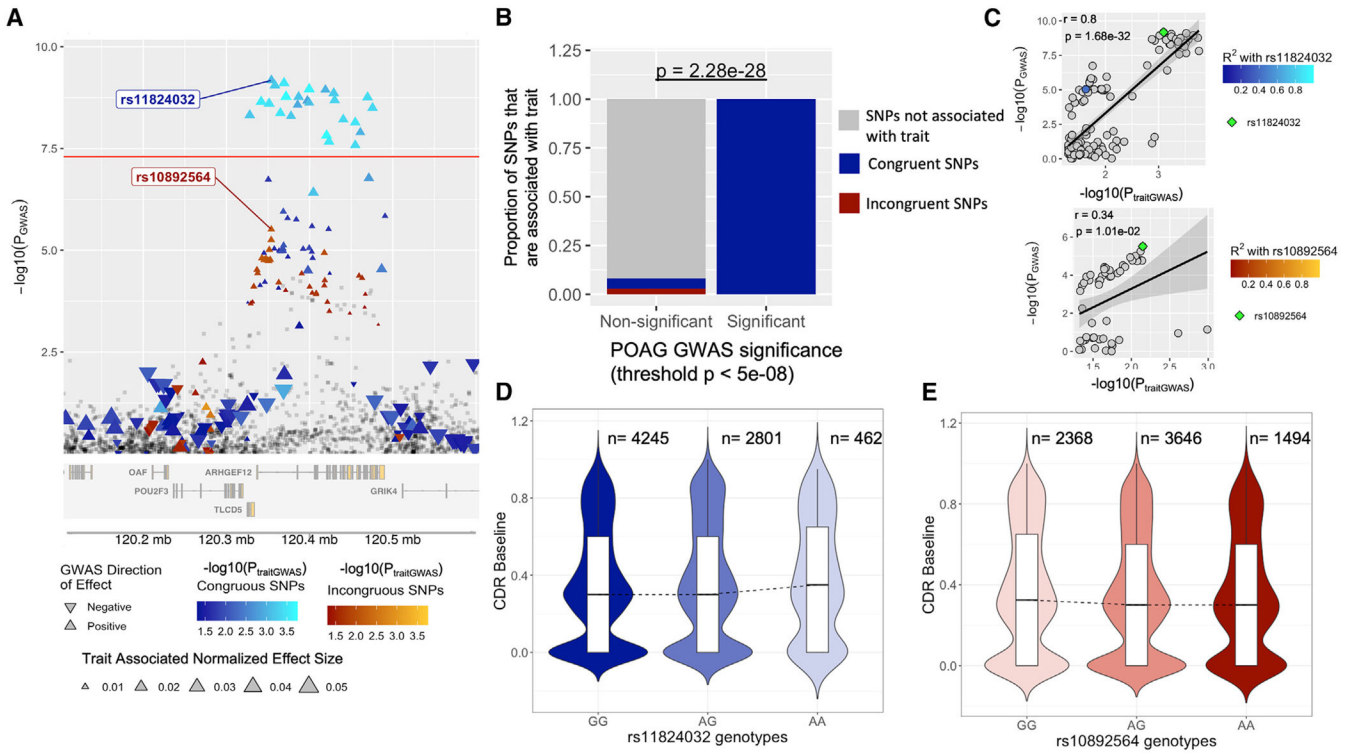

Figure 3. Trait co-localization results

(A) Mega-analysis of discovery cohort, colored by trait GWAS data for baseline CDR, with separation of congruent SNPs (increased expression associated with increase in the trait) versus incongruent SNPs (increase in expression associated with a decrease in the trait).

(B) Enrichment of SNPs associated with baseline CDR among significant SNPs from the mega-analysis.

(C) P-P plot, with congruent SNPs on top and incongruent SNPs at the bottom.

(D) Violin boxplot, with rs11824032 genotypes on the x axis and baseline CDR on the y axis.

(E) Violin boxplot, with rs10892564 genotypes on the x axis and baseline CDR the on the y axis.

See also Table S5.

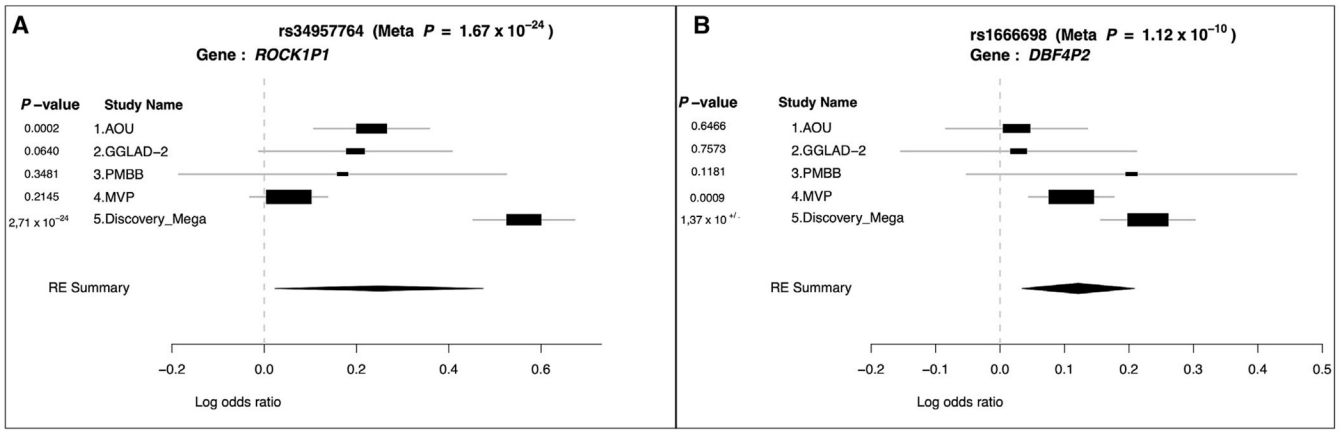

Figure 4. Forest plot showing effect estimates for discovery mega-analyses and replication studies, as well as the pooled effect meta-analyses for two replicated risk variants

Pooled estimates for odds ratio and 95% confidence intervals of all replication datasets and meta-analyses (discovery + all replication sets) were calculated by random effect analyses. Results for individual datasets are denoted by rectangles with lines indicating the 95% confidence intervals and black diamonds indicating the final pooled summary values. All replication datasets include GGLAD-2 + PMBB + AOU + MVP datasets. Meta-analyses p values calculated from the ForestPM plot package are denoted on the top of each plot.

(A) SNP rs34957764 in the *ROCK1P1* gene was tested in all datasets.

(B) SNP rs1666698 in the *DBF4P2* gene was tested in all datasets.

GGLAD-2, Genetics of Glaucoma in People of African Descent; PMBB, Penn Medicine BioBank; AOU, All of Us; MVP, Million Veteran Program.

See also Table S6 and Figures S2 and S3.

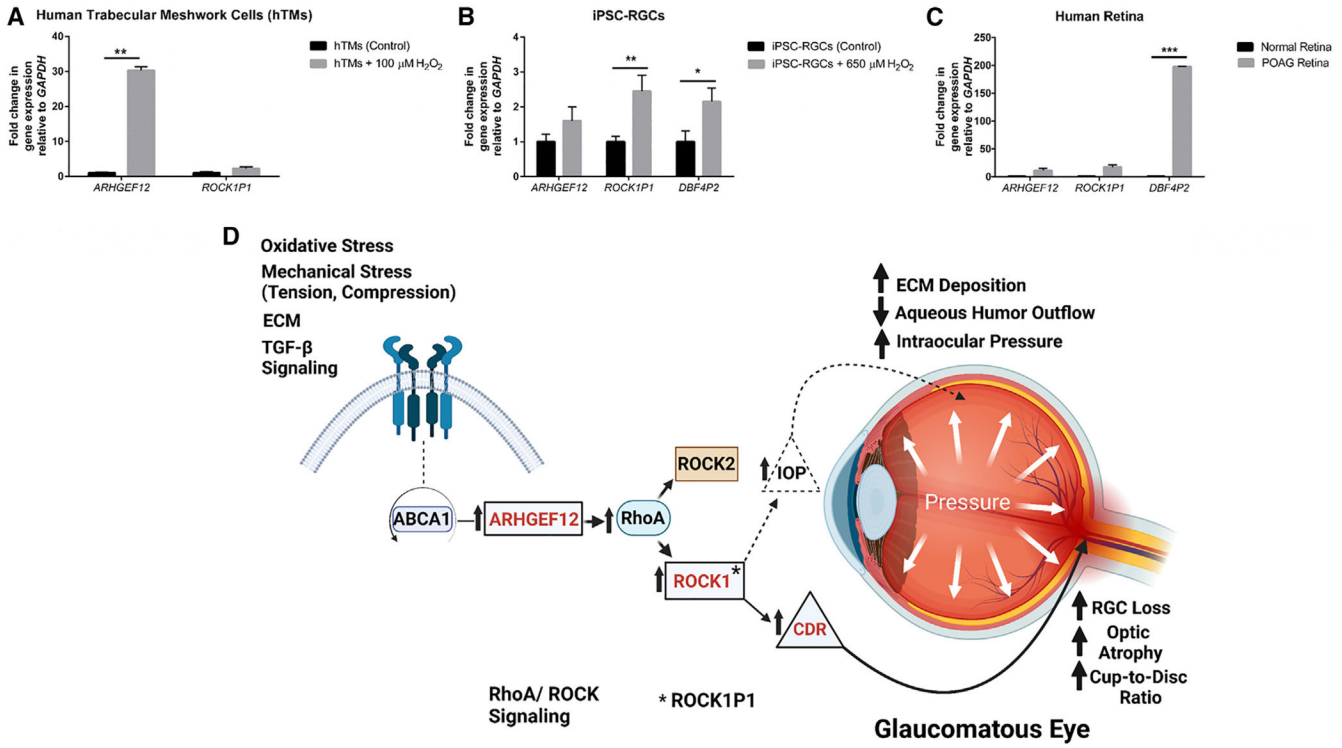

Figure 5. Quantitative gene expression analyses results and proposed mechanisms of genes

Solid arrows indicate the proposed mechanisms of variants identified in our dataset and dashed arrows indicate a mechanism that is known in the literature.

**ROCK1P1* is a pseudogene and is a result of the partial duplication of the *ROCK1* gene. A variant that maps to *ROCK1P1* was identified in our discovery mega-analysis and replicated in the AOU dataset.

The quantitative expression profiles of the nearest genes to the three likely causal variants from the mega-analysis (*ARHGEF12, ROCK1P1*, and *DBF4P2*) were analyzed in human eye tissues (hTMs, iPSC-RGCs, and retinal cells) using quantitative RT-PCR, with and without H_2O_2 treatment.

(A) hTMs were treated with or without 100 μM H_2O_2.

(B) iPSC-RGCs were treated with or without 650 μM H_2O_2.

(C) Human retinal tissues from normal and glaucoma donors were used. *GAPDH* was used as the housekeeping gene. Data are presented as mean ± SEM. The data were normalized to control cells and analyzed using Student's t test statistical analysis (*$p < 0.05$, **$p < 0.01$, ***$p < 0.001$).

(D) Schematic representation of RhoA/ROCK downstream signaling pathway involving ARHGEF12 and ROCK1 and leading to glaucoma in individuals of African ancestry. We propose that ARHGEF12 functions downstream of the TGF-β and RhoA/Rho-associated kinase signaling pathways to activate ROCK1 via RhoA, which decreases TM plasticity and aqueous humor outflow and increases RGC death and optic nerve atrophy.

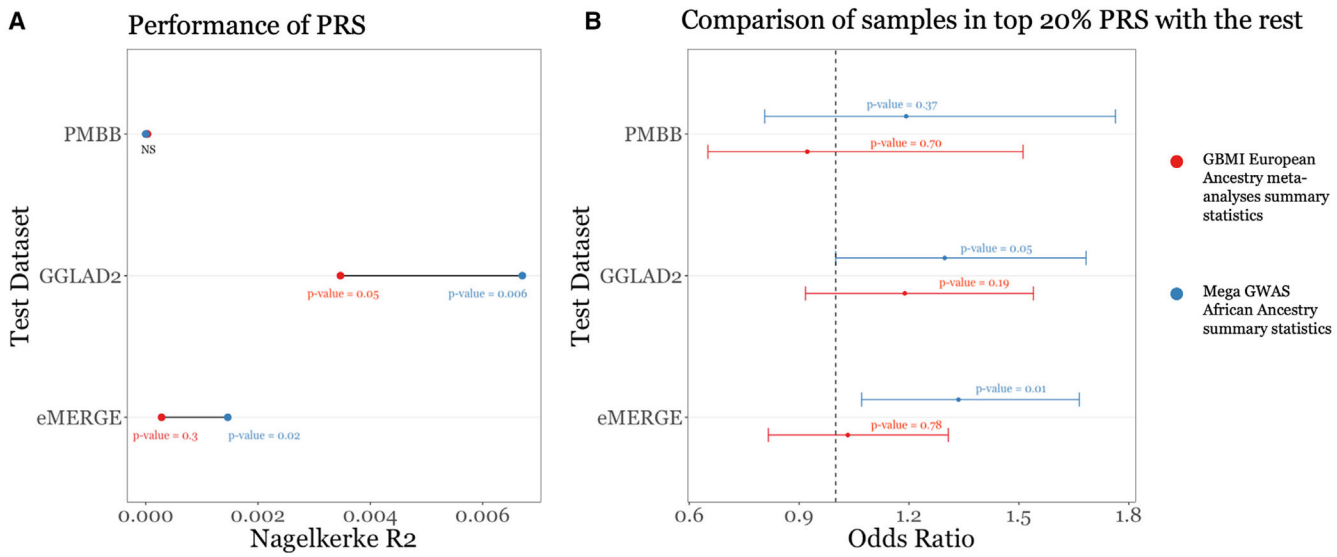

Figure 6. Performance of PRS generated from summary statistics from GBMI (European individuals) and the discovery mega-analysis (African individuals) in independent datasets of African ancestry individuals

Summary statistics from GBMI (European individuals) and discovery mega-analysis (African individuals) were each used to create a PRS. Each PRS was measured in three independent datasets of African ancestry individuals (eMERGE, GGLAD-2, PMBB).

(A) The Nagelkerke R^2 is shown on the x axis, and the test datasets are shown on the y axis, with the p value corresponding to the Nagelkerke p value.

(B) The odds ratio (x axis) was calculated by comparing individuals in top 20% PRS with rest of the test datasets (y axis). The p value corresponds to regression p value.

See also Table S8.

Table 1.

Genome-wide significant loci from the mega-analysis in discovery cohorts

Chr:Position	Lead variant rsID	Nearest gene	Effect allele	Non-effect allele	Allele frequency	OR	Lower limit 95% CI	Upper limit 95% CI	p value
1:146895002	rs36172683	*LOC124900456*	T	G	0.79	1.67	1.51	1.86	5.2E–23
1:1557146	rs4320726	*SSU72*	C	T	0.08	1.42	1.25	1.61	3.5E–08
1:192888862	rs1231753	*RN7SKP126*	G	A	0.94	0.61	0.53	0.72	4.4E–10
1:197079478	rs35655718	*ASPM*	T	C	0.49	0.81	0.75	0.86	7.9E–10
1:53756898	rs1183394	*LOC124904179*	A	G	0.93	1.63	1.39	1.91	6.2E–10
10:28988113	rs17755250	*LOC124403927*	A	C	0.18	1.33	1.22	1.44	3.6E–12
10:39164667	rs879082727	*CHEK2P5*	A	G	0.79	1.38	1.23	1.56	3.7E–08
10:47323706	rs4922508	*GDF2*	A	G	0.86	0.56	0.49	0.64	8.5E–18
10:48058038	rs1308452687	*RNA5SP315*	T	A	0.83	0.70	0.63	0.78	9.9E–11
11:120354080	rs11824032	*ARHGEF12*	G	A	0.25	1.24	1.16	1.33	6.6E–10
11:121138670	rs34002948	*TECTA*	G	A	0.66	1.32	1.23	1.42	2.1E–14
11:50385050	rs117353933	*LINC02750*	G	A	0.05	0.47	0.39	0.58	3.3E–13
11:54708680	rs4611187	*OR4A5*	T	C	0.06	0.60	0.51	0.70	9.6E–11
12:127391021	rs57347531	*LINC02375*	G	T	0.06	0.68	0.60	0.79	3.7E–08
12:128365235	rs74537852	*TMEM132C*	C	T	0.08	0.67	0.59	0.75	2.9E–11
12:70810380	rs1040027	*PTPRR*	C	T	0.56	1.26	1.18	1.34	2.7E–13
12:7783972	rs6488629	*LOC108942766*	T	C	0.92	1.67	1.43	1.95	4.8E–11
13:23420079	rs4770444	*SACS*	G	T	0.92	0.72	0.64	0.81	4.9E–08
14:105708459	rs144145908	*IGH*	C	T	0.09	1.50	1.33	1.68	3.7E–12
14:31624055	rs28580449	*NUBPL*	C	T	0.38	1.23	1.15	1.31	1.6E–09
14:56502862	rs4584747	*LOC101927690*	A	C	0.53	1.25	1.17	1.34	1.5E–11
15:100159652	rs145914721	*ADAMTS17*	T	C	0.06	0.62	0.54	0.71	4.2E–12
15:25437859	rs77631699	*UBE3A*	A	G	0.02	2.67	2.04	3.49	4.2E–13
16:33823269	rs720126	*IGHV3OR16-13*	C	T	0.34	1.34	1.21	1.47	2.4E–09
16:5113716	rs7189371	*ENPP7P14*	G	C	0.88	0.70	0.62	0.78	4.9E–10
17:83183702	rs71193787	*LOC101929650*	T	A	0.30	1.40	1.29	1.51	4.6E–17
18:15232752	rs9963245	*BNIP3P3*	A	G	0.45	1.45	1.33	1.58	1.5E–16

Chr:Position	Lead variant rsID	Nearest gene	Effect allele	Non-effect allele	Allele frequency	OR	Lower limit 95% CI	Upper limit 95% CI	p value
18:93327	rs34957764	*ROCK1P1*	C	T	0.10	1.75	1.97	1.56	4.9E–24
19:6832739	rs73000309	*VAV1*	T	C	0.05	1.63	1.39	1.90	3.6E–10
2:111570643	rs1666698	*DBF4P2*	T	C	0.63	0.80	085	0.74	3.6E–10
2:88849801	rs141848863	*LOC108348023*	C	T	0.06	0.61	0.53	0.71	3.9E–11
20:62675278	rs4809477	*SLCO4A1*	T	C	0.75	0.80	0.75	0.86	1.7E–09
22:19485902	rs5746749	*CDC45*	A	C	0.94	0.66	0.57	0.75	1.2E–09
3:125210558	rs671064	*SLC12A8*	G	A	0.89	1.36	1.22	1.52	2.2E–08
4:189790415	rs2739537	*FRG1-DT*	T	C	0.87	1.50	1.32	1.70	4.2E–10
4:42192281	rs139976752	*BEND4*	C	A	0.09	1.40	1.25	1.57	6.0E–09
4:51830626	rs9998449	*DCUN1D4*	A	G	0.64	1.33	1.22	1.46	6.9E–11
6:191736	rs9502903	*LOC285766*	A	G	0.69	1.41	1.30	1.53	2.2E–16
6:3176138	rs369229648	*TUBB2BP1*	C	T	0.03	0.53	0.44	0.65	7.0E–10
6:88968505	rs6939237	*RNGTT*	A	G	0.96	0.60	0.50	0.72	8.3E–09
7:4048923	rs6462562	*SDK1*	A	G	0.46	1.22	1.14	1.30	1.8E–09
7:73913547	rs55701129	*LOC121740686*	T	C	0.05	1.52	1.32	1.76	3.8E–09
8:101852942	rs534512	*NCALD*	A	G	0.64	1.23	1.14	1.32	1.0E–08
8:12323125	rs34536966	*DEFB130A*	G	A	0.73	0.75	0.67	0.83	1.1E–08
8:68235044	rs11556027	*PREX2*	C	T	0.87	1.47	1.32	1.63	3.8E–13
9:131033574	rs3780279	*LAMC3*	A	C	0.93	0.71	0.63	0.81	4.2E–08

KEY RESOURCES TABLE

REAGENT or RESOURCE	SOURCE	IDENTIFIER
Biological samples		
Eye tissues obtained from normal and glaucoma eye donors	Lions Eye Institute for Transplant and Research	N/A
Chemicals, peptides, and recombinant proteins		
Basic fibroblast growth factor (bFGF)	R&D Systems	Cat#: 233-FB
Matrigel growth factor (GFR)	Corning	Cat#: 354230
XAV939 (X) (Wnt inhibitor)	R&D Systems	Cat#: 3748
SB431542 (SB) (TGF-β inhibitor)	R&D Systems	Cat#: 1614
LDN193189 (L) (BMP inhibitor)	R&D Systems	Cat#: 6053
Nicotinamide	Sigma-Aldrich	Cat#: N0636
IGF1	R&D Systems	Cat#: 291-G1
Follistatin 300	R&D Systems	Cat#: 669-FO
Cyclopamine	R&D Systems	Cat#: 1623/1
DAPT	Stemgent	Cat#: 04-0041
Y-27632 dihydrochloride (ROCK inhibitor)	R&D Systems	Cat#: 1254/1
Forskolin	Selleckchem	Cat#: S2449
N^6,2'-O-Dibutyryladenosine 3', 5'-cyclic monophosphate sodium salt (cAMP)	Sigma-Aldrich	Cat#: D0627
BDNF	R&D Systems	Cat#: 248-BDB
NT4	R&D Systems	Cat#: 268-N4
CNTF	R&D Systems	Cat#: 257-NT
Critical commercial assays		
Direct-zol RNA Miniprep kits	Zymo Research	Cat#: R2050
SuperScript™ III First-Strand cDNA Synthesis System	ThermoFisher Scientific	Cat#: 18080051
TaqMan™ Fast Advanced Master Mix	ThermoFisher Scientific	Cat#: 4444557
Deposited data		
Genotype data for POAAGG participants	dbGaP	Accession phs001312
Genotype data for ADAGES participants	dbGaP	Accession phs001673
Genotype data for GGLAD participants	Hauser et al.[37]	https://s3-ap-southeast-1.amazonaws.com/gis-hg4-poag/poag_africa_4_collection_logistic.meta.sorted_N4.tsv.zip
Genotype data for AOU participants	All of Us Research Hub	https://databrowser.researchallofus
Genotype data for PMBB participants	N/A	Accessed via collaborations with researchers upon request.
Genotype data for MVP participants	N/A	Accessed via collaborations with researchers upon request.
Genotype data for GBMI participants	GBMI Initiative Website	https://www.globalbiobankmeta.org/resources.

REAGENT or RESOURCE	SOURCE	IDENTIFIER
eMERGE Phase III data	dbGaP	Accession phs001584.v2.p2
HapMap variants	1000 Genomes FTP portal	http://ftp.ncbi.nlm.nih.gov/hapmap/genotypes/2009-01_phaseIII/plink_format/.
NHGRI-EBI GWAS catalog	Welter et al.[43]	https://www.ebi.ac.uk/gwas/
Quantitative gene expression analysis (Figure 6)	Mendeley Data	https://doi.org/10.17632/7drg5smn9j.1
Experimental models: Cell lines		
Primary trabecular meshwork cells	Commercially obtained from Sciencell, CA, USA and laboratory of Dr. Markus Kuehn, University of Iowa.	Cat#6590
Human: Undifferentiated induced pluripotent stem cells (iPSCs)	UPenn iPSC Core	N/A
Software and algorithms		
TOPMED Imputation Reference Panel	Das et al.[39]	https://imputation.biodatacatalyst.nhlbi.nih.gov/#!
EIGENSOFT package	Galinsky et al.[101,102]	http://www.hsph.harvard.edu/alkes-price/software
SAIGE version 1.1 software	Mbatchou et al.[103]	https://saigegit.github.io/SAIGE-doc/
R (Version 3.6.3)	N/A	https://cloud.r-project.org/bin/windows/base/old/3.6.3/R-3.6.3-win.exe
LocusZoom web interface.	Boughton et al.[104]	https://github.com/statgen/locuszoom/
LDSC software	Zheng et al.[105]; Bulik-Sullivan[106]	http://ldsc.broadinstitute.org/; https://github.com/bulik/ldsc/
GCTA-COJO software	Yang et al.[44]	http://gump.qimr.edu.au/gcta/massoc.html
PLINK	Chang et al.[107]	https://www.cog-genomics.org/plink/2.0/general_usage
Popcorn (version 1.0)	Brown et al.[52]	https://github.com/brielin/popcorn
SuSie in PolyFun (POLYgenic FUNctionally informed fine-mapping	Weissbrod et al.[56]	https://github.com/stephenslab/susieR
GraphPad Prism 6.0	N/A	https://www.graphpad.com/dl/96314/10B92408/
EpIMAP	Li et al.[54]	https://epigenomegateway.wustl.edu/
MAGMA (Multivariate Analysis of Genomic Annotation) tool	Watanabe et al.[65]; de Leeuw et al.[66]	http://ctglab.nl/software/magma.
Other		
Human Eye Transcriptome Atlas	Wolf et al.[70]	https://www.eye-transcriptome.com